Optical Theory of Image Scanning Microscopy

Colin Sheppard
Italian Institute of Technology (IIT)
Genoa, Italy
colinjrsheppard@gmail.com

Molecular Horizons
School of Chemistry and Molecular Biosciences,
University of Wollongong, Australia

Two ways to form an image

Full-field detection

detector array

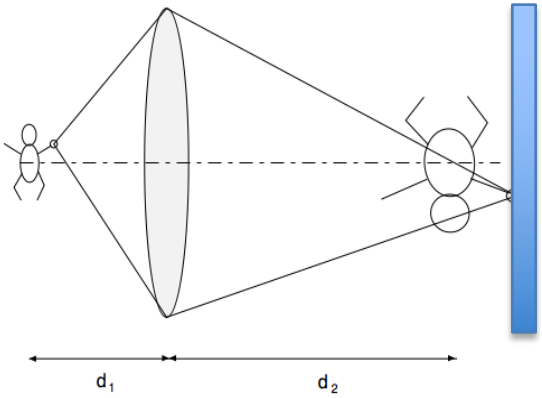

Scanning system

single element detector

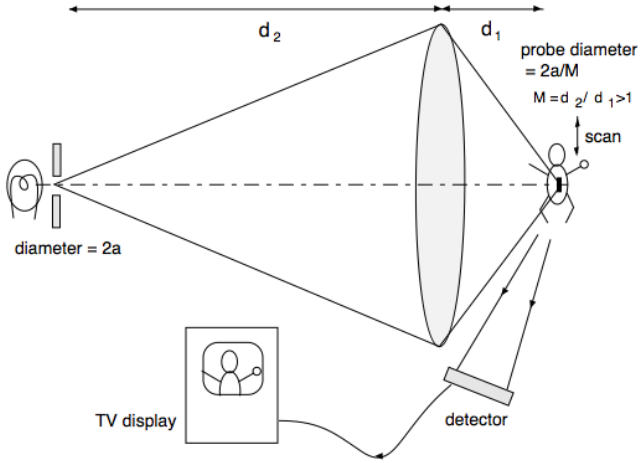

OPTICA ACTA, 1977, VOL. 24, NO. 10, 1051–1073

Image formation in the scanning microscope

C. J. R. SHEPPARD and A. CHOUDHURY

CHAPTER 1

The Generalized Microscope*

COLIN J. R. SHEPPARD

School of Physics, and Australian Key Centre for Microscopy and Microanalysis, The University of Sydney, NSW 2006, Australia

*This chapter is based upon an invited presentation at the Symposium of the Australian Society for Electron Microscopy, University of Sydney, 1996.

Confocal and Two-Photon Microscopy: Foundations, Applications, and Advances, Edited by Alberto Diaspro.
ISBN 0-471-40920-0

Combine these:

4D signal $I(x_1,y_1; x_2,y_2)$:

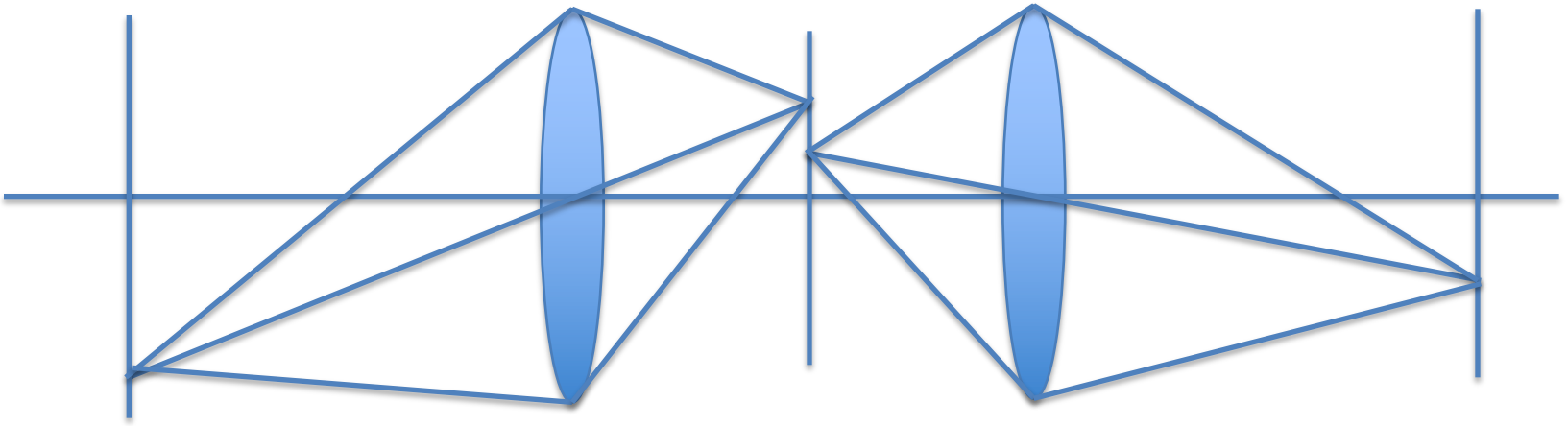

Confocal case, $x_1 = x_2$; $y_1 = y_2$:

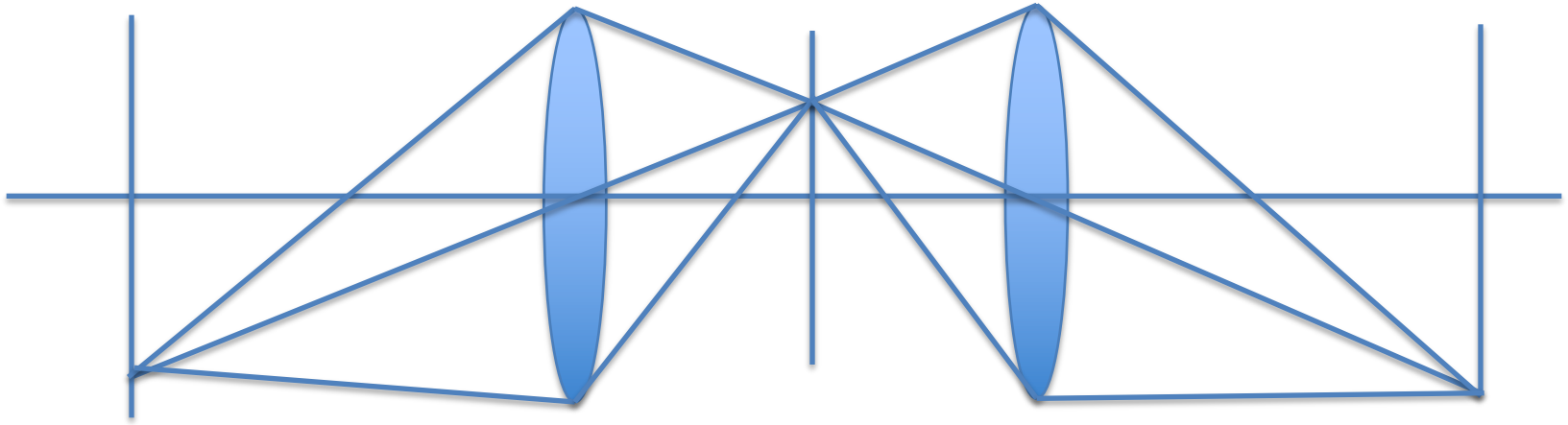

Scanning vs. conventional microscope

Conventional

Conventional with image scanning

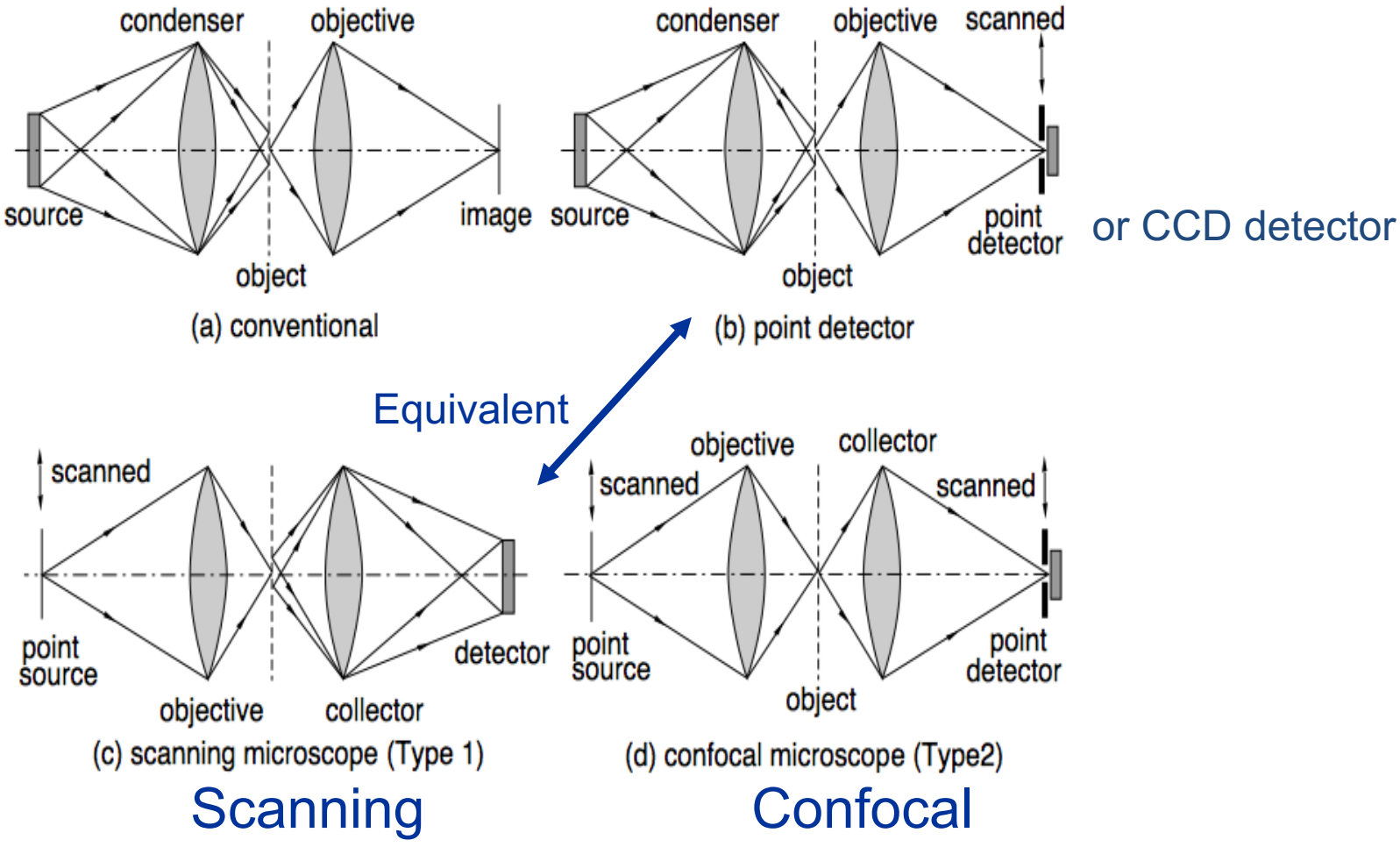

Scanning

Confocal

Confocal microscopy

- Advantages
  - Optical sectioning
    - 3D imaging
    - Surface profiling
  - Reduced scattered light
    - Imaging through scattering media, e.g. tissue
  - Improved resolution (for small pinhole)
- Reflection
  - Industrial applications, surface profiling
  - Scattering media, tissue (**non-invasive**)
- Fluorescence
  - Autofluorescence or labelled
  - Fixed or living

Confocal Imaging (non-fluorescence)

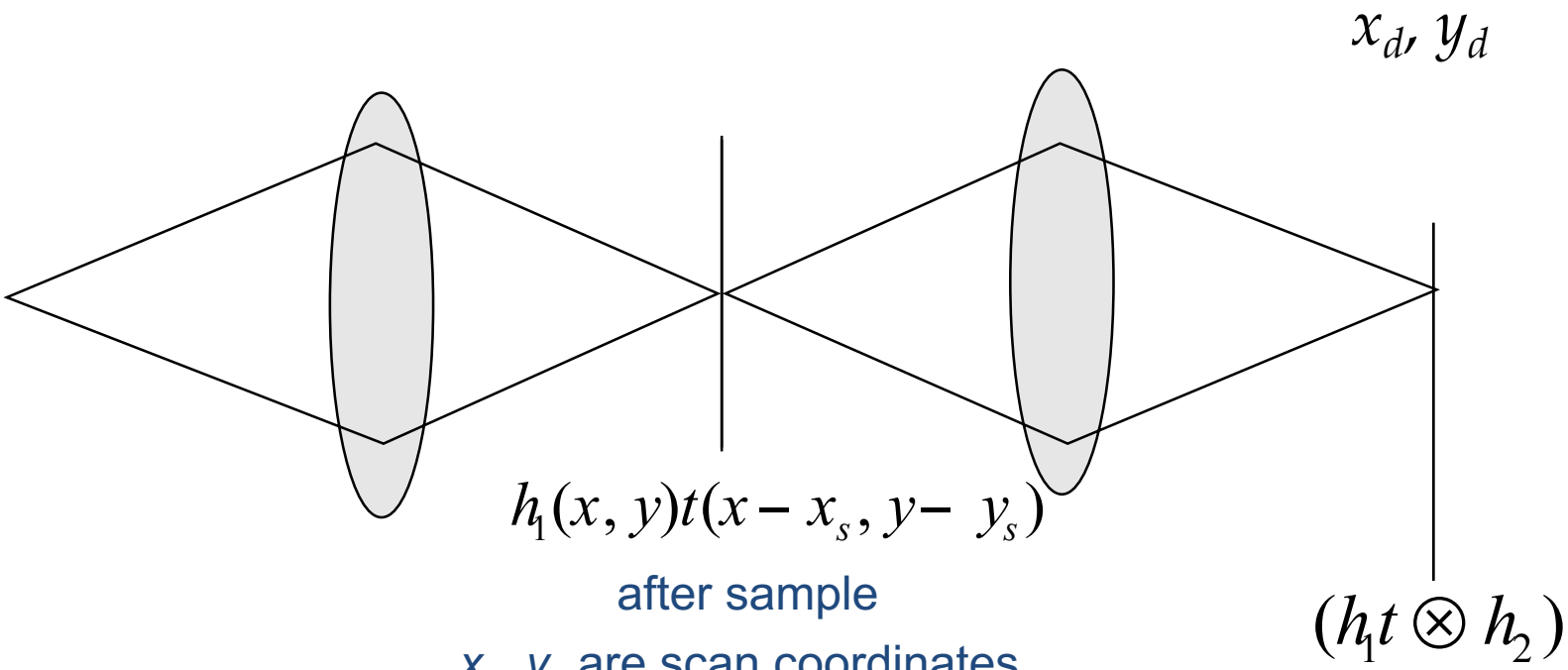

$$I(x_d, y_d) = \left| \iint h_1(x,y)t(x-x_s, y-y_s)h_2(x_d-x, y_d-y)\,dx\,dy \right|^2$$

- Pinhole: $x_d, y_d = 0$:

$$I = \left| \left(h_1(x,y)h_2(-x,-y)\right) \otimes t(x,y) \right|^2$$

- h_2 even:

$$I = \left| (h_1 h_2) \otimes t \right|^2$$

  - Same as coherent microscope, with $h_{eff} = h_1 h_2$
  - Transfer function is convolution of c_1 with c_2

Integrated intensity

Integrated intensity: transverse integral of the point spread function.

Integrated intensity falls off monotonically with distance from the focal plane, as $1/z^2$.

The normalized distance for it to fall to ½ of the in-focus value, $u_{1/2}$, is a measure of the optical sectioning strength.

The integrated intensity is the same as the image of a fluorescent sheet, so for a uniform fluorescent background, integration over a thick volume converges.

u is axial optical coordinate $8n\pi z\,(\sin\alpha/2)^2/\lambda$

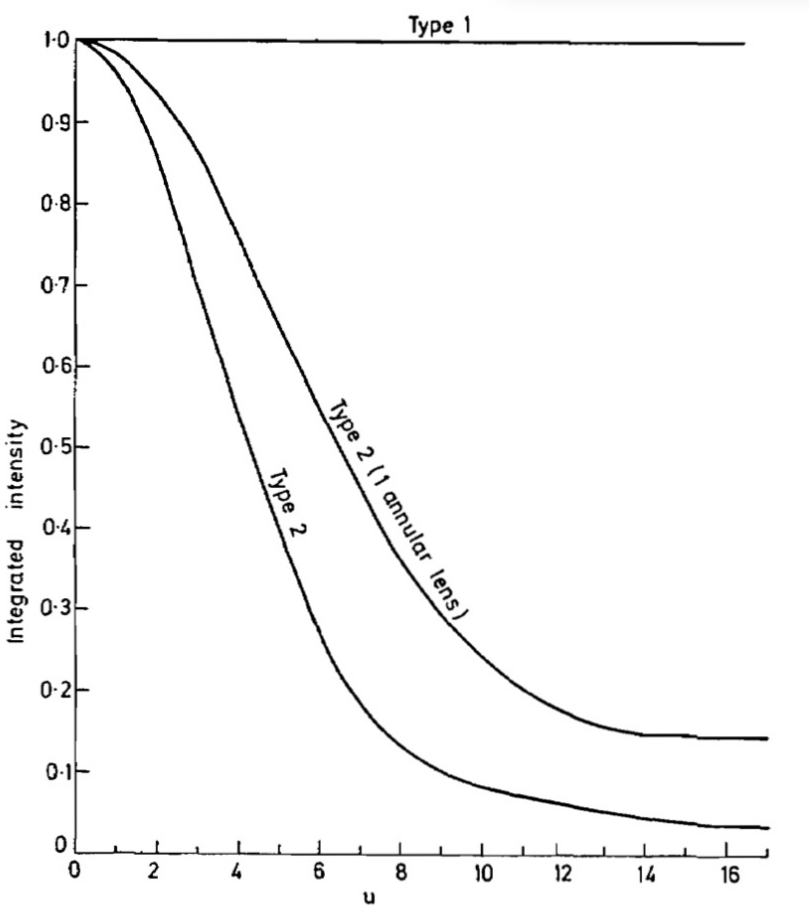

Fig. 1. The variation in the integrated intensity in the image of a single-point normalized distance u from the focal plane of the microscope for a scanning microscope of Type 1 and for scanning microscopes of Type 2 with two circular pupils, and with one circular and one annular pupil.

Depth of field in the scanning microscope

September 1978 / Vol. 3, No. 3 / OPTICS LETTERS 115

C. J. R. Sheppard and T. Wilson

OTF for confocal fluorescence

Cut-off doubled but response is very weak

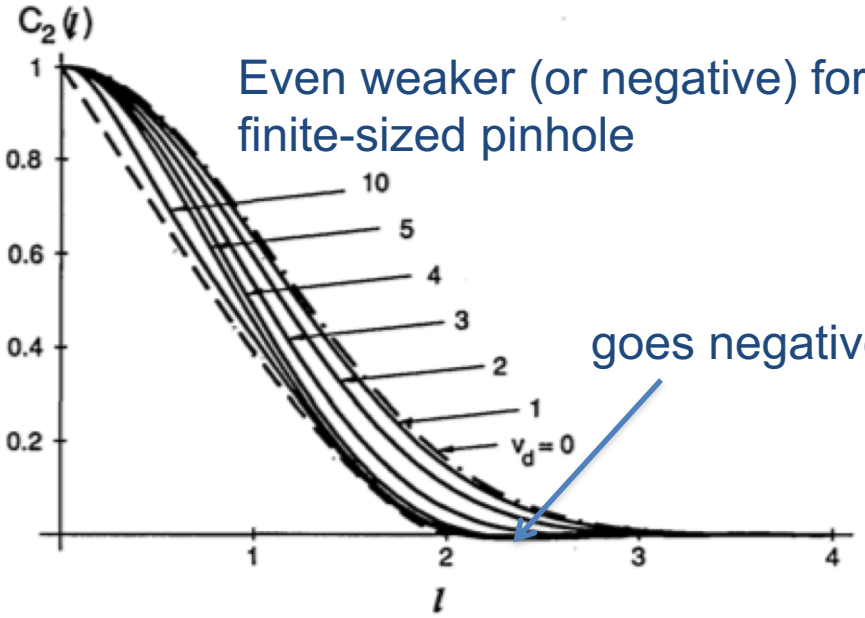

Even weaker (or negative) for finite-sized pinhole

goes negative!

Fig. 4. Normalized in-focus (2-D) OTF for different radii of the detector. The dashed curve represents the 2-D OTF when $v_d \to \infty$.

Plot suggests possibility to use pupil filters to increase the magnitude of the OTF!

Optik 60, No. 4 (1982) 391–396 © Wissenschaftliche Verlagsgesellschaft mbH, Stuttgart

Super-resolution by confocal fluorescent microscopy

JOSA Communications Vol. 9, No. 1/January 1992/J. Opt. Soc. Am. A 151

Confocal fluorescent microscopy with a finite-sized circular detector

Min Gu and C. J. R. Sheppard

Main problem: Finite sized pinhole

- Need finite sized pinhole to get adequate signal
- Then resolution improvement is lost

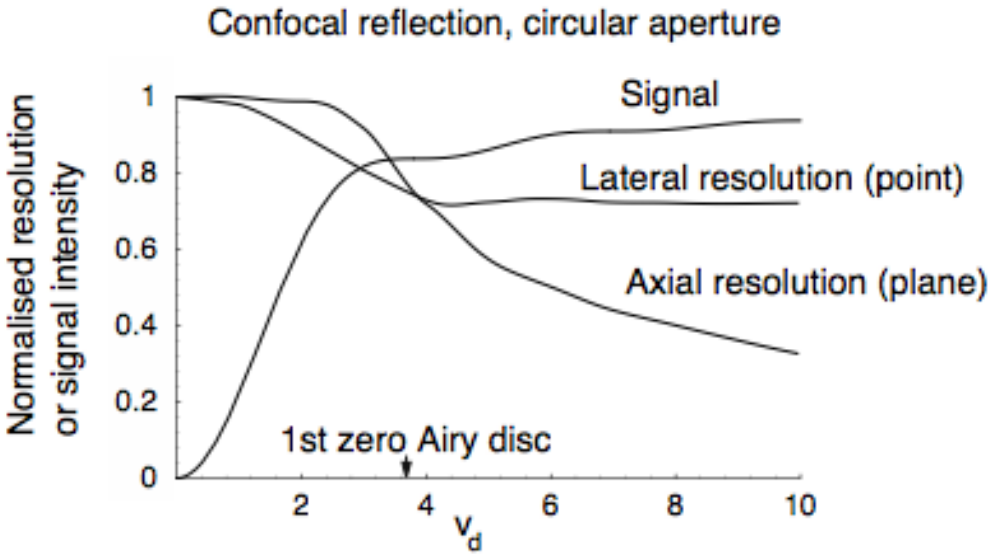

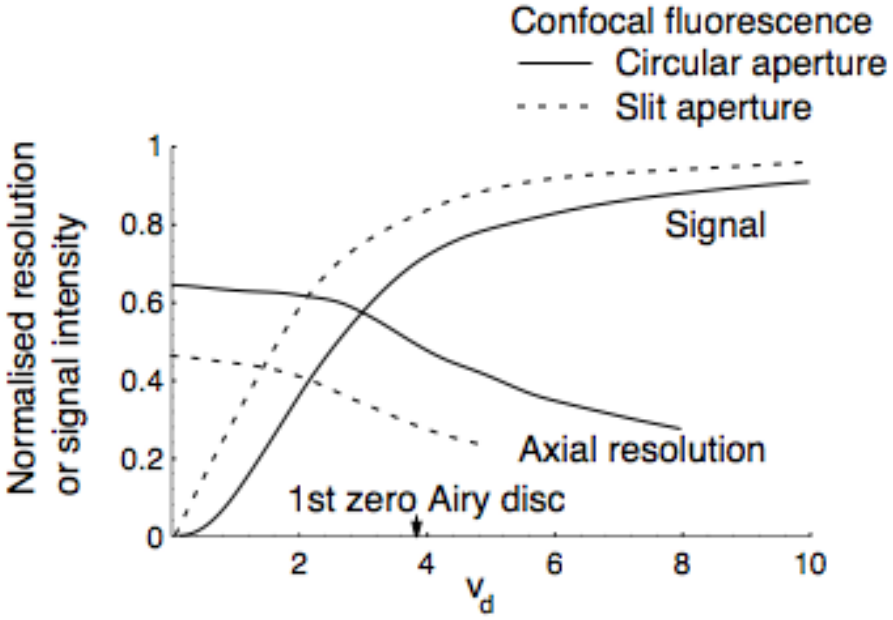

v is lateral optical coordinate ($n\pi r \sin\alpha$) /λ

CJR Sheppard and DM Shotton
Confocal Laser Scanning Microscopy,
RMS, Bios, and Springer, 1997

Illumination and detector arrays

Detector array in image plane

- Structured illumination (Lukosz, 1963; Gustafsson, 2000)
- Tandem scanning (spinning disc) (Petrán, 1968)
- Singular value decomposition with detector array (Bertero & Pike, 1982)
- 'Type 3' : Maximum signal in detector plane (Reinholz, 1987)
- Pixel reassignment (Sheppard, 1988)
- Subtractive imaging (Wilson,1984 ; Cogswell & Sheppard, 1990 + many others)
- Video confocal microscopy (Benedetti, 1996)
- Programmable array microscope PAM (Hanley 1999, Verveer 1998)
- Structured illumination + nonlinear (Heintzmann, 2002; Gustafsson)
- Structured detection, J Lu, Concello, Xie, Lichtmann (2009);RW Lu, Biomed Opt Exp (2013)
- Computational nonlinear scanning (CNS) microscopy (Laporte, Optica (2014))

Offset pinhole

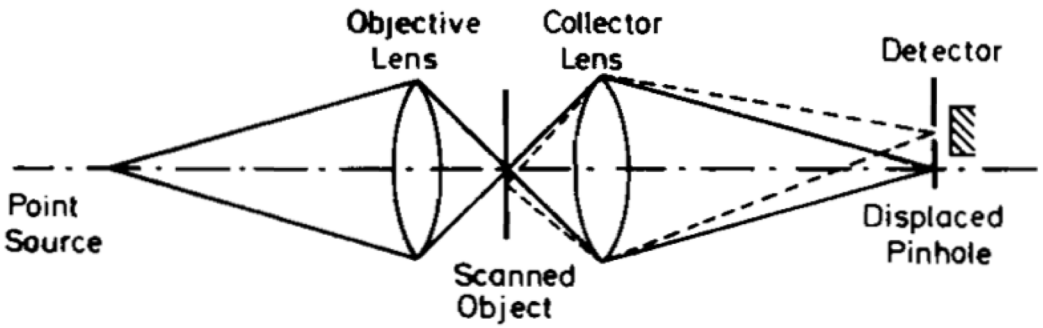

PSF:

$$I(v) = \left[\frac{2J_1(v-\bar{v})}{v-\bar{v}}\right]^2 \left[\frac{2J_1(v+\bar{v})}{v+\bar{v}}\right]^2$$

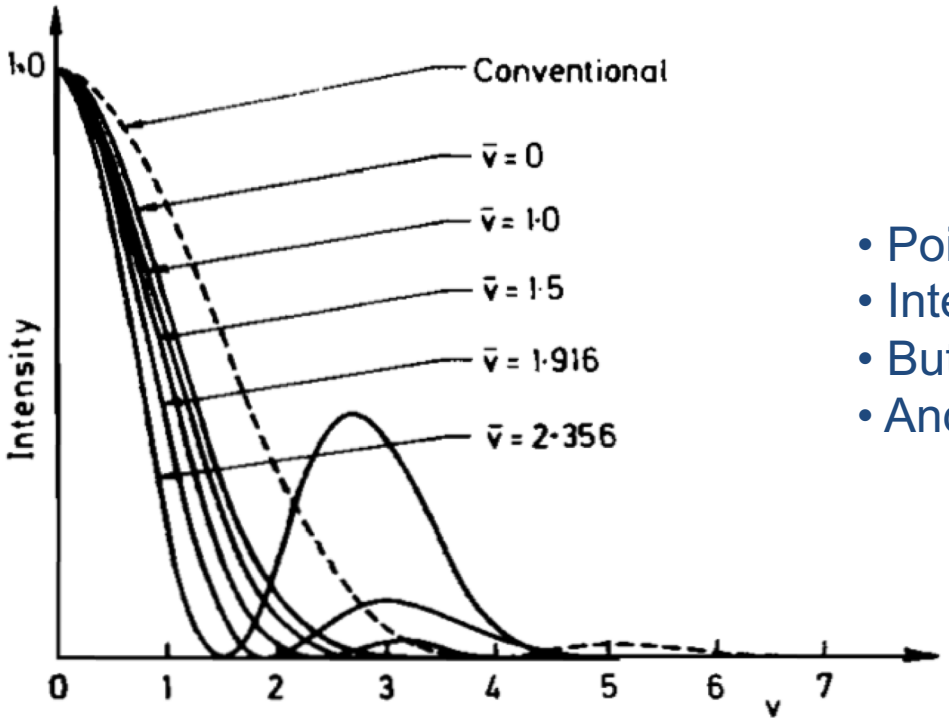

- Point spread function gets narrower
- Intensity decreases
- But increased side lobes
- And effective psf shifts sideways

Improvement in resolution by nearly confocal microscopy

APPLIED OPTICS, Vol. 21, page 778, March 1, 1982

I. J. Cox, C. J. R. Sheppard, and T. Wilson

Gives the image of a shifted object point

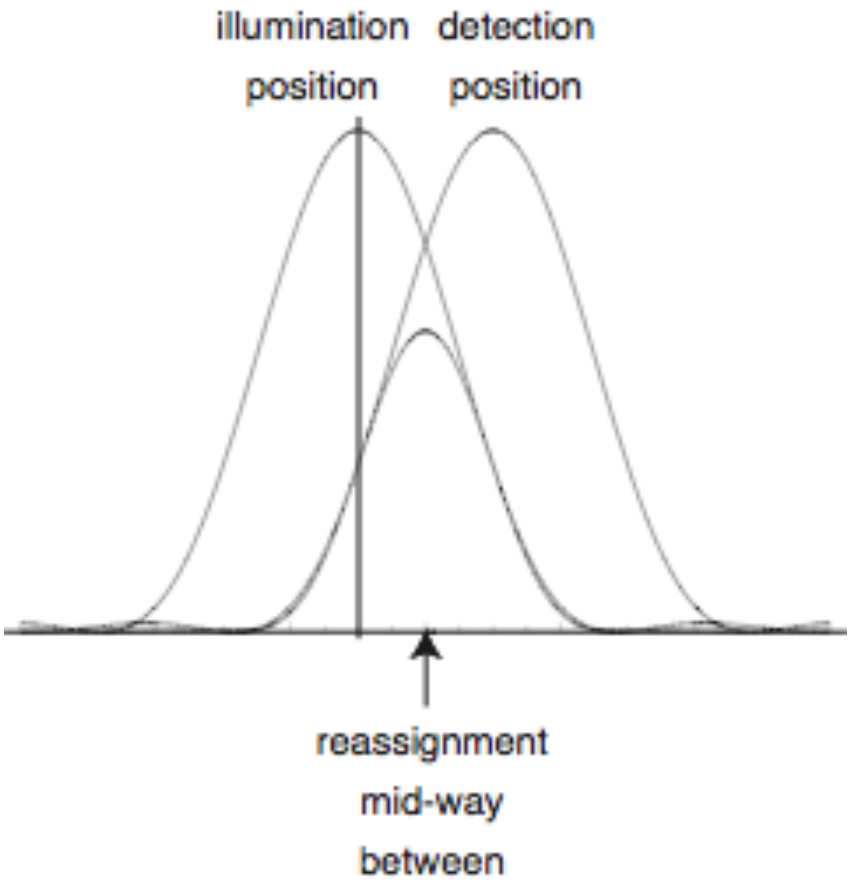

Offset pinhole & reassignment

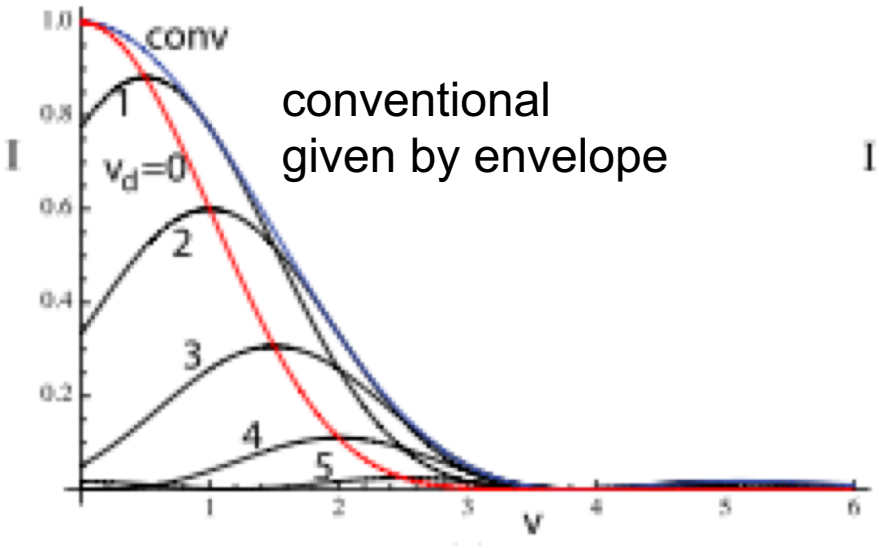

offset pinhole

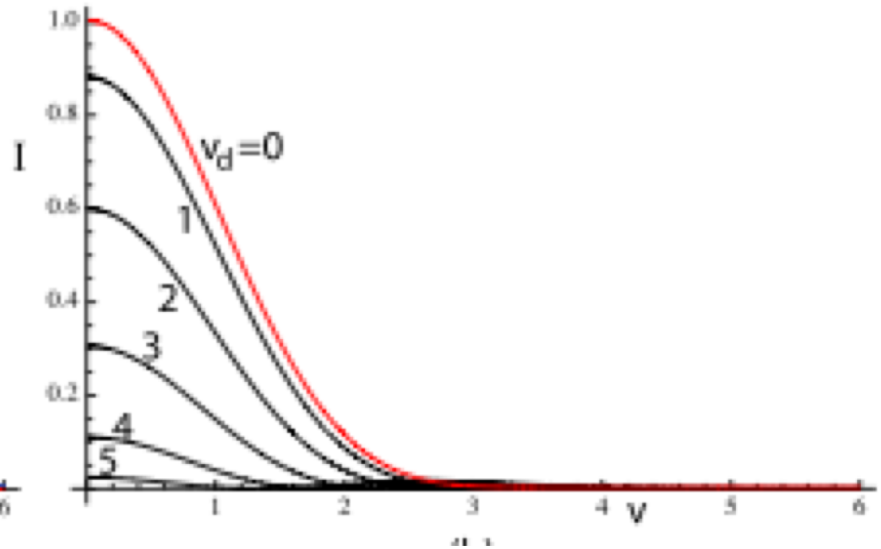

after reassignment

- Integrate without reassignment: same as conventional
- Integrate with reassignment (to centre of illumination and detection):
  PSF sharpened and signal improved

Pixel reassignment

Abstract

A new explanation for the imaging improvement of confocal microscopy is presented. A method of further increasing the imaging performance is also discussed.

function of $2x_s$

convolution of rescaled PSFs
(not **product** of PSFs
as for confocal)

$$I(x_s) = \{|h_1|^2 \otimes |h_2|^2\}(2x_s)$$

Optical transfer function

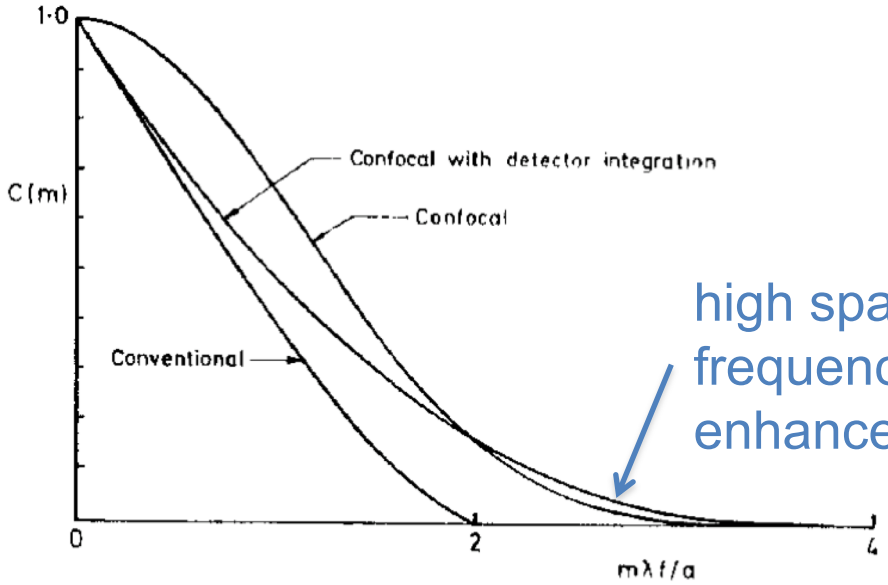

Fig. 2. Incoherent transfer functions for a fluorescence microscope. The radius of the circular pupils is a.

high spatial frequencies enhanced

$$C(m) = \{(P_1 \otimes P_1^*)(P_2 \otimes P_2^*)\}(m\lambda f/2)$$

$OTF_1 \times OTF_2$

product of rescaled OTFs
(not **convolution** of OTFs
as for confocal)

Super-resolution in Confocal Imaging

C. J. R. Sheppard,

Optik 80, No. 2 (1988) 53 54

Image scanning microscopy

PRL 104, 198101 (2010)

Selected for a Viewpoint in *Physics*
PHYSICAL REVIEW LETTERS

Image Scanning Microscopy

Claus B. Müller and Jörg Enderlein*

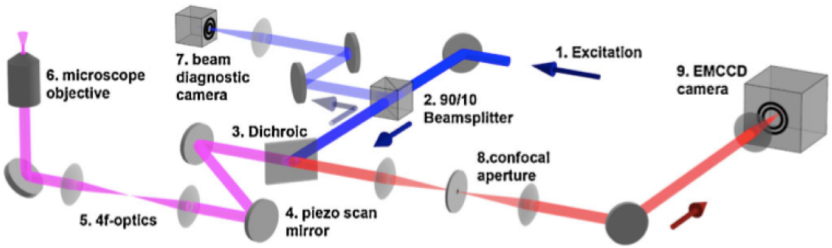

FIG. 1 (color online). ISM Setup, (1) Excitation with supercontinuum white light source and acousto-optic tunable filter, (2) 90/10 nonpolarizing beam splitter cube, (3) major dichroic mirror, (4) piezo scan mirror, (5) 4f telescope, (6) UPL APO 60x W microscope objective, (7) beam diagnostic camera, (8) confocal aperture, and (9) EM CCD detection camera system.

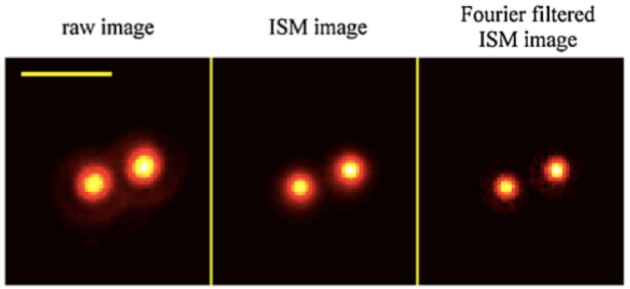

FIG. 2 (color online). Image of a single fluorescent bead of 100 nm diameter. Left panel: CLSM image; middle panel: ISM image; right panel: Fourier-weighted ISM image. The horizontal bar in the left panel has a length of 1 μm.

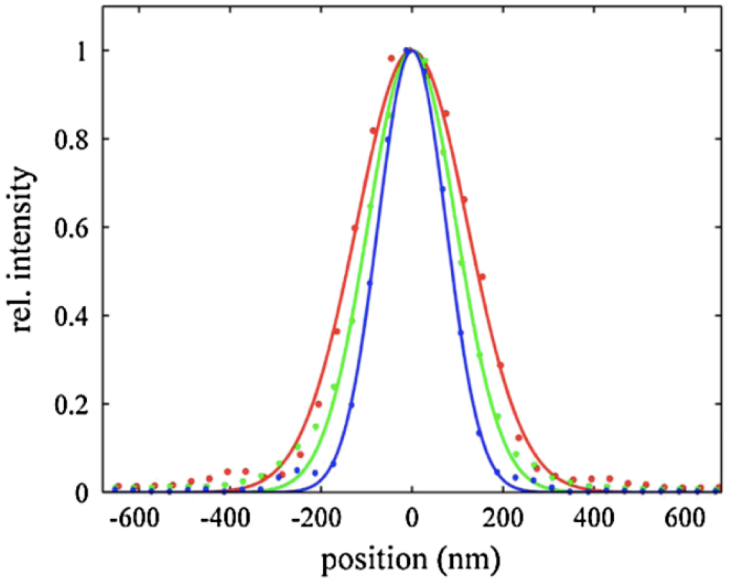

Optical sectioning

But, for v_{dmax} ➔ ∞, no optical sectioning!
Need to limit size of array

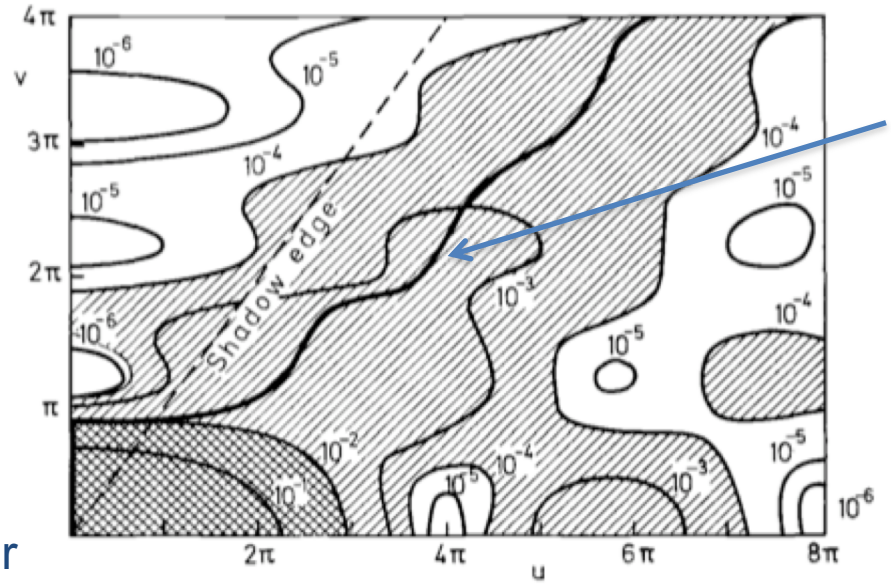

points on detector array > 0.72 AU, image regions away from the focal plane

v = 2.747

(0.72 AU) magic number

Figure 4. The intensity in the confocal image of a single point. The locus of the auto-focus scan of the image is also shown. The cross-hatched region is that in which the intensity is greater than 0·01. The corresponding region for a conventional system is shown shaded.

Locus of u_{Imax} (v)

JOURNAL OF MODERN OPTICS, 1988, VOL. 35, NO. 1, 145–154

The extended-focus, auto-focus and surface-profiling techniques of confocal microscopy

C. J. R. SHEPPARD and H. J. MATTHEWS

Integration over finite detector array

peak intensity goes above 1!

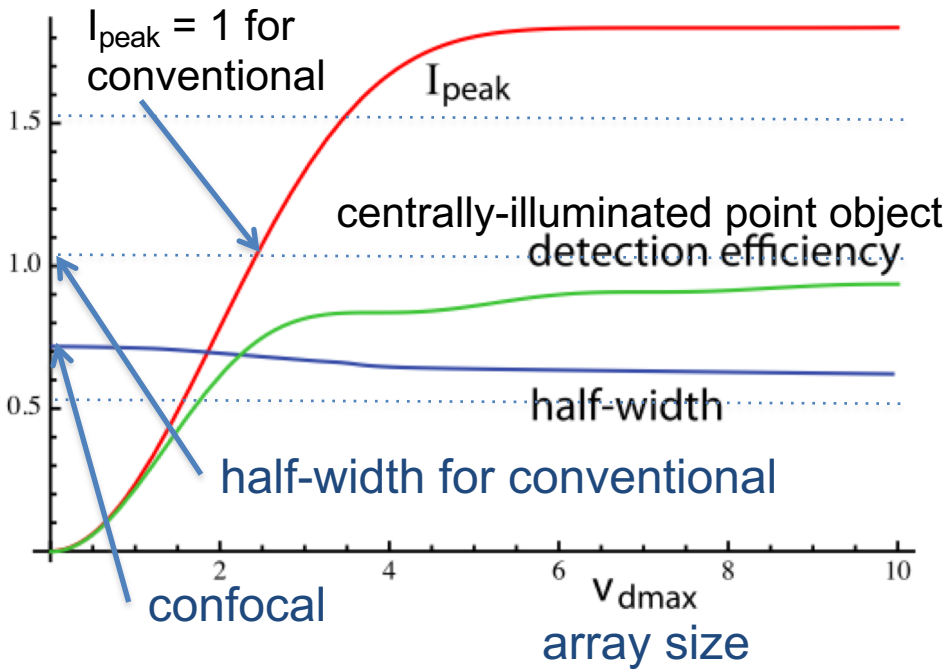

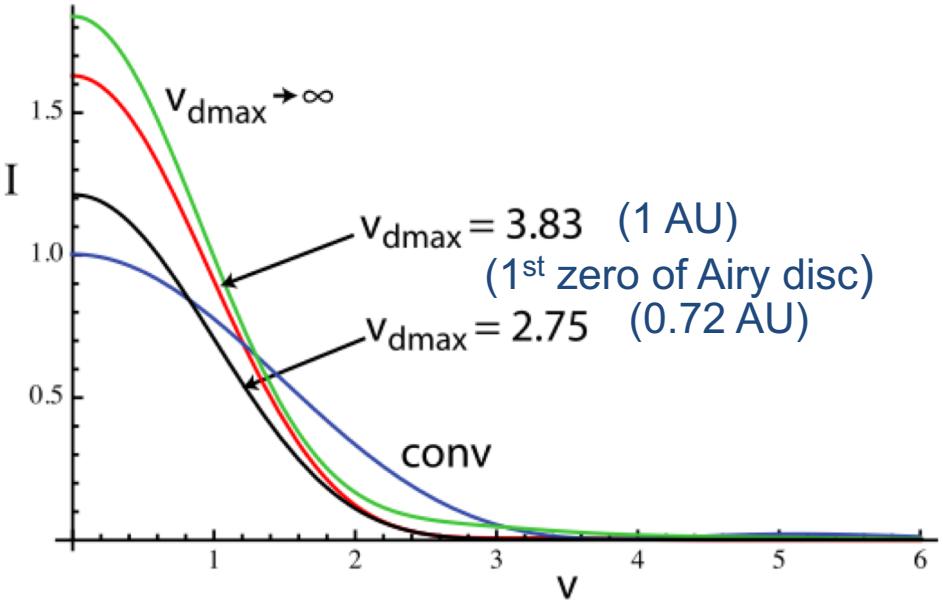

- Peak is >1!
- Super-concentration
- Beats classical limit of etendue
- But integrated intensity is independent of reassignment

Resolution and signal strength improve as size of array (v_{dmax}) increases

Peak of point spread function for large array is $4(1-16/3\pi^2) = 1.84$

(4 elements gives ~1.4)

August 1, 2013 / Vol. 38, No. 15 / OPTICS LETTERS 2889

Superresolution by image scanning microscopy using pixel reassignment

Colin J. R. Sheppard,[1,*] Shalin B. Mehta,[2] and Rainer Heintzmann[3,4,5]

Image of a point object: Effect of array size

Width of psf does not change much with array size, but tail does change

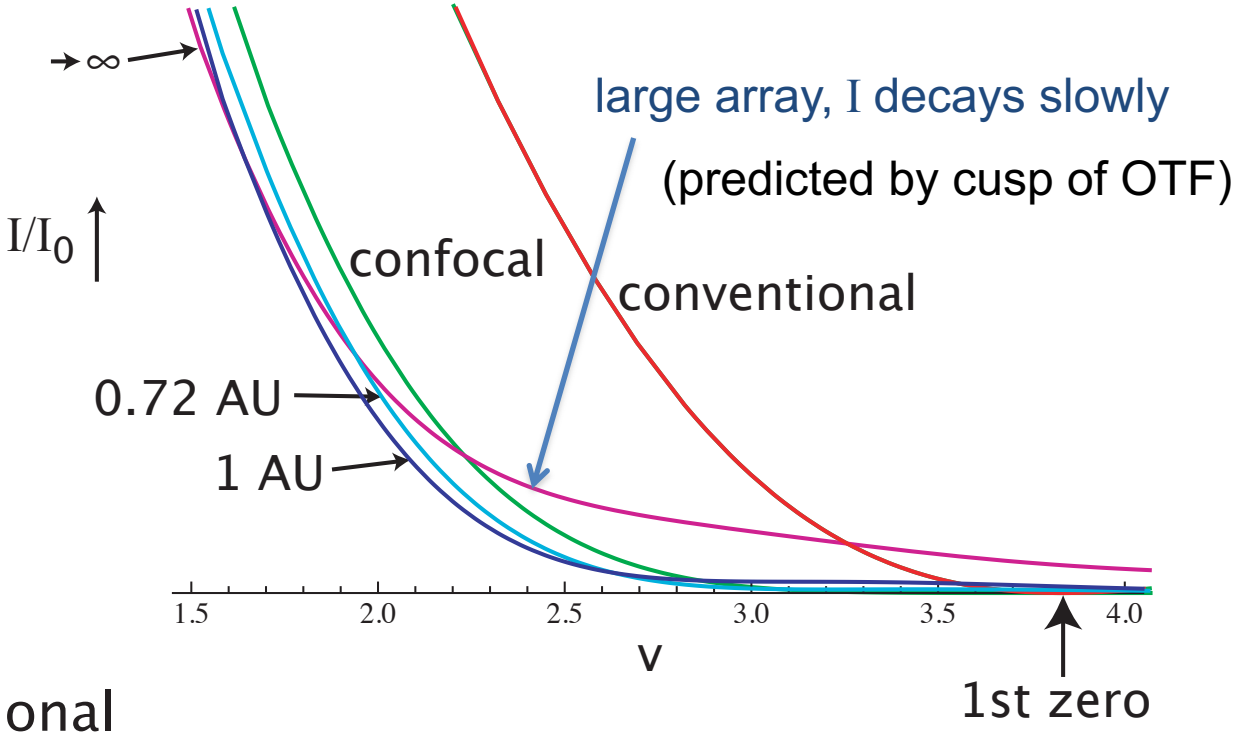

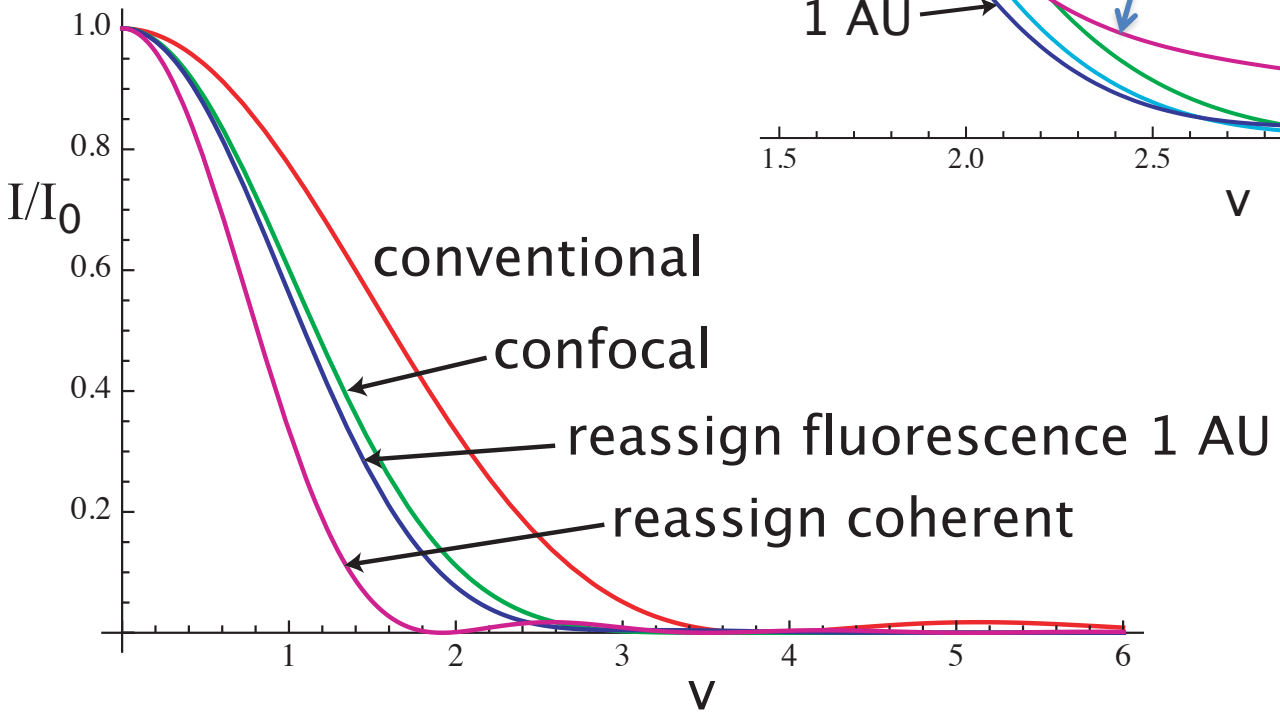

Unnormalized OTF for confocal and ISM

For unnormalized OTF, $C(0)$ gives signal from a fluorescent sheet

confocal with finite pinhole

ISM with finite detector array

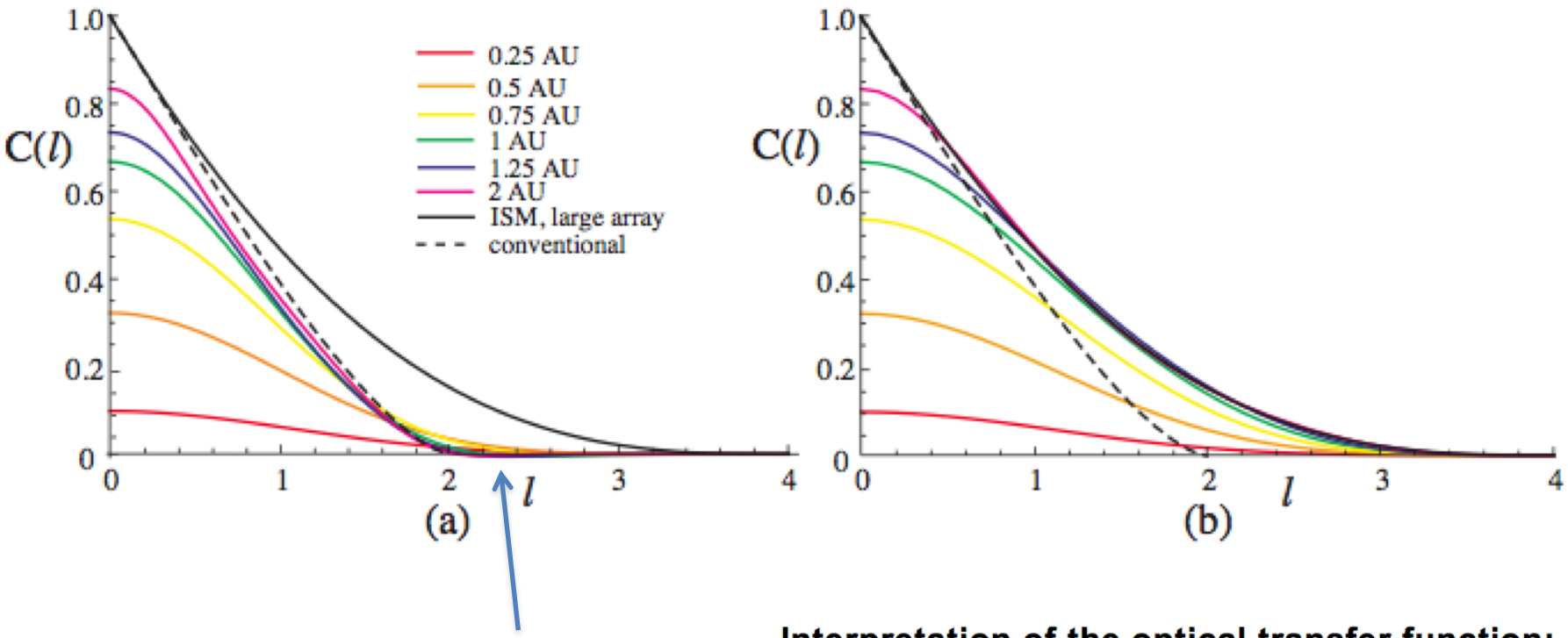

goes negative!

Interpretation of the optical transfer function: Significance for image scanning microscopy

COLIN J. R. SHEPPARD,[1*] STEPHAN ROTH,[2,3] RAINER HEINTZMANN,[2,3] MARCO CASTELLO,[1,4] GIUSEPPE VICIDOMINI,[1] RUI CHEN,[5] XUDONG CHEN,[5] AND ALBERTO DIASPRO[1,4,6]

Opt. Express 24(24), 27280-27287 (2016)

General microscope with source/detector arrays

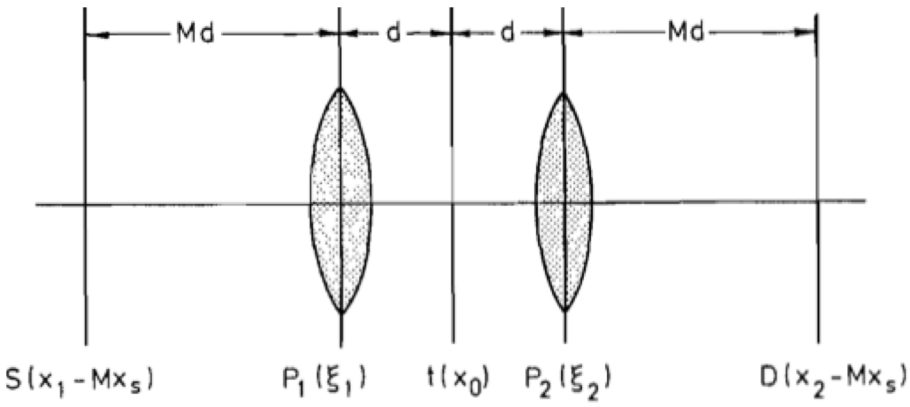

Journal of Microscopy, *Vol.* 124, *Pt* 2, *November* 1981, *pp.* 107–117.
Revised paper accepted 10 *March* 1981

The theory of the direct-view confocal microscope

by C. J. R. SHEPPARD *and* T. WILSON, *University of Oxford, Department of Engineering Science, Parks Road, Oxford*

Intensity as a function of scanning position and detector position

4D signal: $I(x_d, y_d; x_s, y_s)$

Microimage: $I(x_d, y_d)$ **for fixed** x_s, y_s

Scanned image: $I(x_s, y_s)$ **for fixed** x_d, y_d

Fluorescence (incoherent), 4D signal is:

$$I(x_1, x_2) = \int H_1(x_1 - x) H_2(x_2 - x) T(x)\, dx$$

Benedetti Video-Confocal Microscope (VCM)

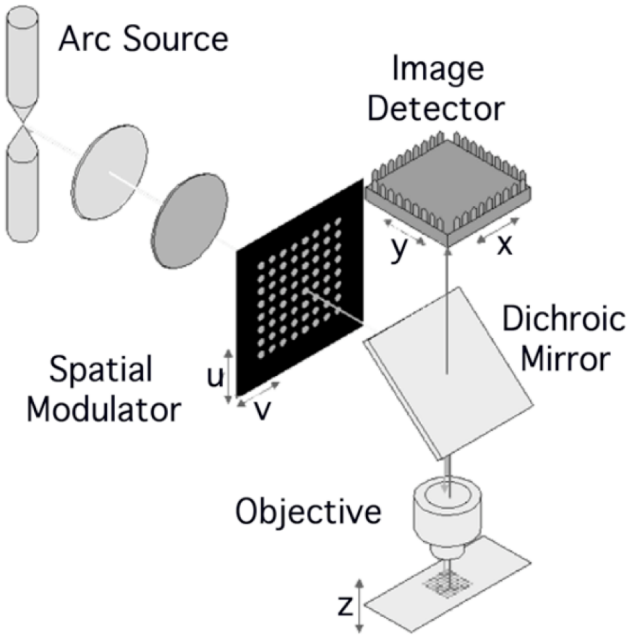

— for each position of the illumination pattern, collecting raw images at a detector comprising light detector elements arranged according to coordinates x,y, each raw image described by a light intensity distribution function $I_{u\,v}(x,y)$ on the image detector;

— computing a final image $I_h(x,y)$ starting from the raw images $I_{u\,v}(x,y)$.

In a first aspect of the invention, the step of computing the final image comprises executing an algorithm configured for calculating, for each light detector element, at least one value of a central moment of order ≥3 of the light intensity distribution, the central moment of order ≥3 having at each coordinate x,y a value that depends upon the asymmetry of the intensity values distribution of each raw image versus the position of the illumination pattern, wherein the central moment is defined as:

$$m_h(x,y)= Avg\{[\, I_{u\,v}(x,y)- Avg(I_{u\,v}(x,y))]^h\}, \qquad [1]$$

wherein: h is an integer number ≥3; $Avg(I_{u\,v}(x,y))$ is the average of the intensity value distribution $I_{u\,v}(x,y)$, i.e. it is equal to $(\sum_{u\,v} I_{u\,v}(x,y))/ (UV)$, u=1 ... U,v=1...V. wherein $Avg(I_{u\,v}(x,y))$ is, for each light detector element of said detector, the average of the intensity obtained for all the positions u,v of said illumination pattern.

This way, the final image takes higher values at the coordinates x,y of the light detector elements that correspond to positions at which critically focused sample portions are present.

In other words, the moments of order h ≥ 3, which are used in the algorithm for computing the final video-confocal image, contain light intensity distribution data that allow to take into account the symmetry/asymmetry degree of the light intensity distribution at each pixel, i.e. at each light detector element of the detector, versus the position u,v of the illumination pattern.

The pixels, i.e. the detector elements of the detector, at which there is a higher asymmetry of the light intensity distribution correspond to sample portions that are critically focused, i.e. they correspond to sample portions that have a higher density, and/or to sample portions that emanate a higher brightness, for instance by fluorescence, by reflection or even by transmission, which points out local unevennesses and specific features of these sample portions.

Therefore, the above-mentioned critically focused sample portions are highlighted as more bright portions in the final confocal image.

Therefore, if central moments of the light intensity distribution are used to calculate the final image, according to the invention, better performances can be achieved than by prior art methods.

”Improved confocal microscopy methods and devices” patent WO2013144891 (2013)

Fourier transform of 4D signal

4D signal

$$I(x_1,x_2)=\int H_1(x_1-x)H_2(x_2-x)T(x)dx$$

4D Fourier transform

$$\tilde{I}(m_1,m_2)=\tilde{H}_1(m_1)\tilde{H}_2(m_2)\tilde{T}(m_1+m_2)$$

Central and difference coordinates

$$m=\frac{m_1+m_2}{2},m'=\frac{m_1-m_2}{2}$$

$$\tilde{I}(m,m')=\tilde{H}_1\left(m+\frac{m'}{2}\right)\tilde{H}_2\left(m-\frac{m'}{2}\right)\tilde{T}(2m)$$

Conventional: $\tilde{H}_1=\delta\left(m+\frac{m'}{2}\right)$

Scanning: $\tilde{H}_2=\delta\left(m-\frac{m'}{2}\right)$

Confocal: $\int dm' \rightarrow \tilde{H}_1\otimes\tilde{H}_2$

Pixel reassignment:

$$m'=0$$

$$\tilde{I}(m,m')=\tilde{H}_1(m)\tilde{H}_2(m)\tilde{T}(2m)$$

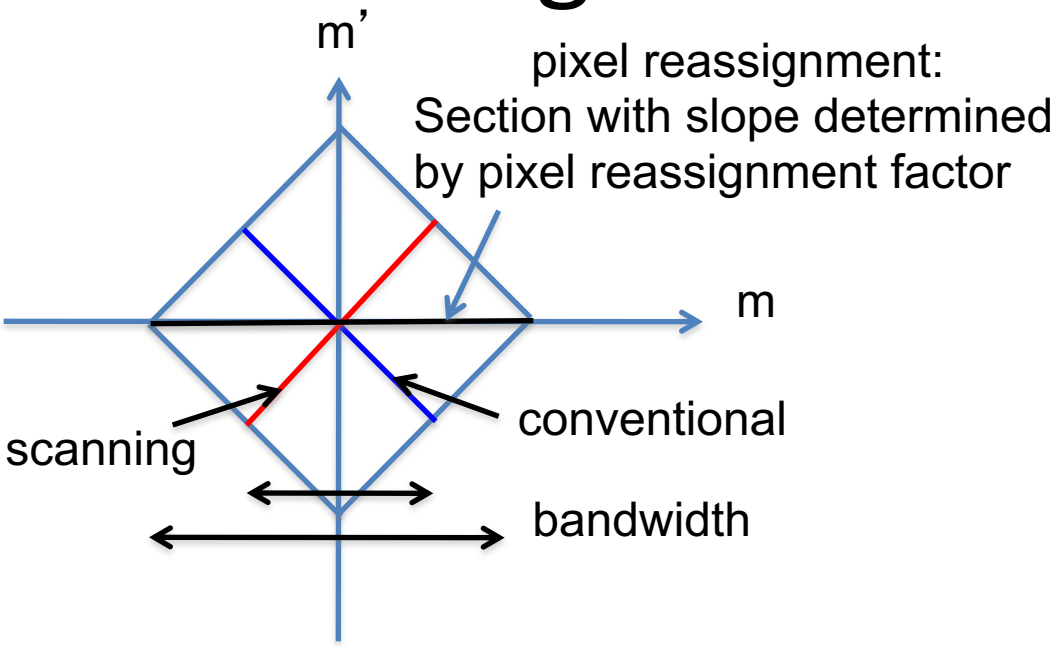

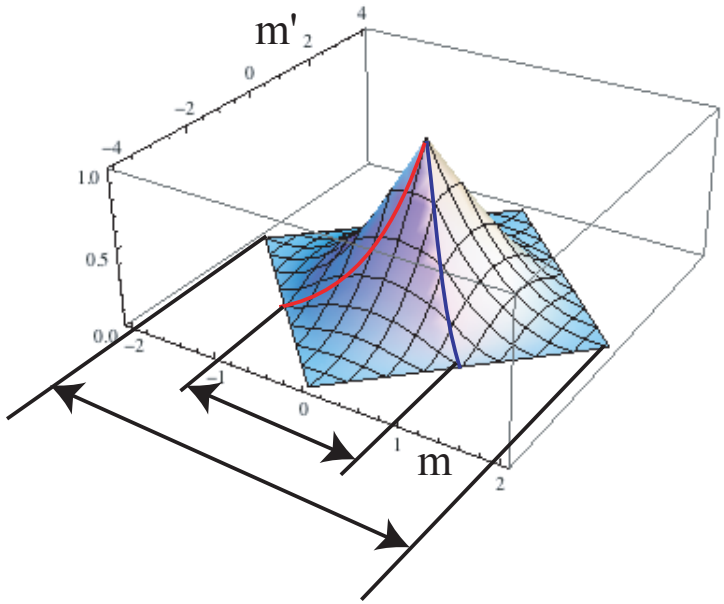

Effect of changing *a*

C(m,m’)

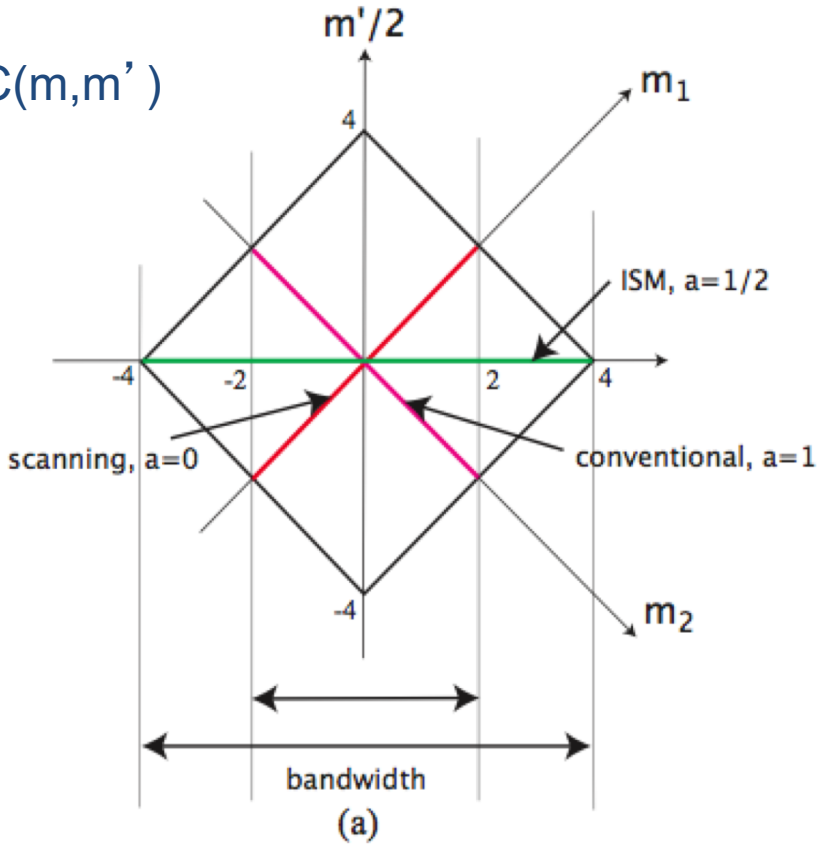

with Stokes shift

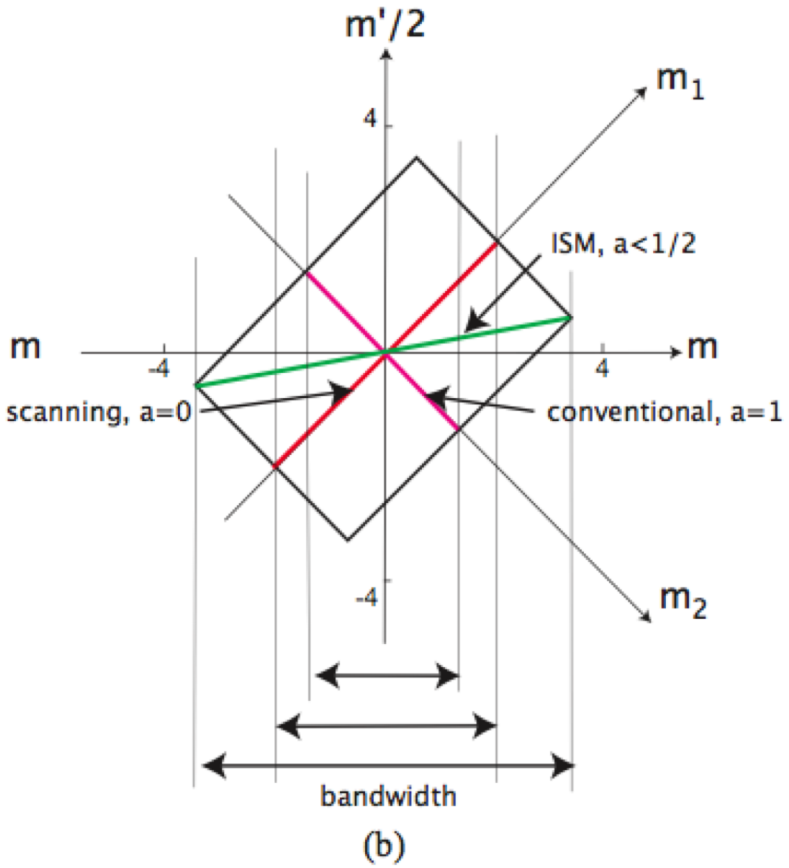

- Changing *a* changes the slope of a line through the origin
- *a*=0 is scanning, *a*=1 is conventional

Research Article Vol. 34, No. 8 / August 2017 / Journal of the Optical Society of America A 1339

Journal of the Optical Society of America A

OPTICS, IMAGE SCIENCE, AND VISION

Image formation in image scanning microscopy, including the case of two-photon excitation

Colin J. R. Sheppard,[1,*] Marco Castello,[1,2] Giorgio Tortarolo,[1,2] Giuseppe Vicidomini,[1] and Alberto Diaspro[1,2,3]

Any reassignment factor *a* is valid

- Can use different reassignment factors *a* for different spatial frequencies
- For a **large** array, OTF is

$$C_{\text{eff}}(l) = C_1[(1-a)l]C_2(al).$$ m

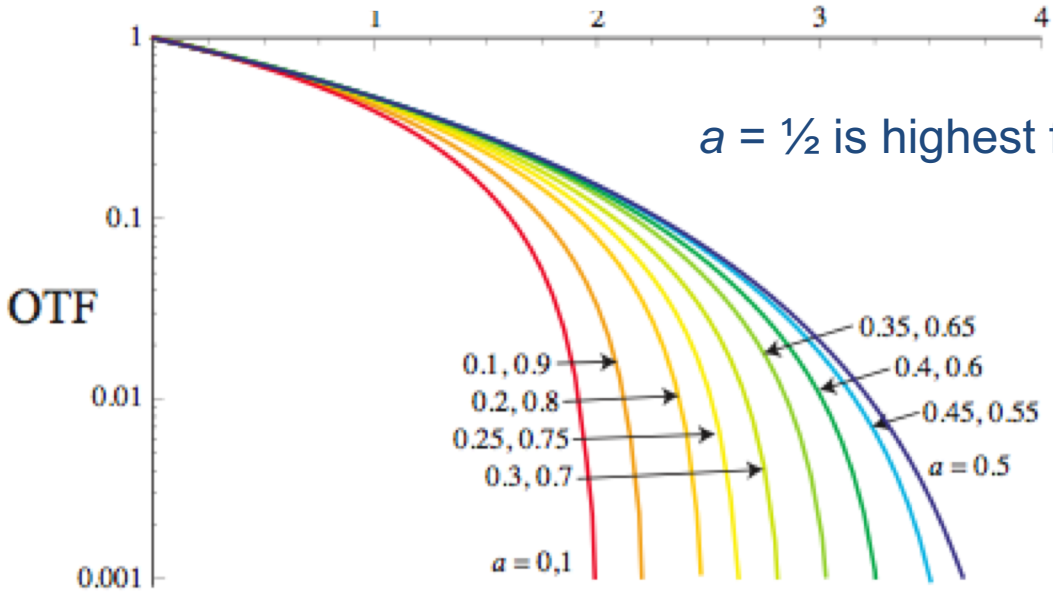

Fig.4. The OTF for 1PE fluorescence ISM with no Stokes shift, for different values of reassignment factor a .

a = ½ is highest for all spatial frequencies

August 1, 2013 / Vol. 38, No. 15 / OPTICS LETTERS 2889

Superresolution by image scanning microscopy using pixel reassignment

Colin J. R. Sheppard,[1,*] Shalin B. Mehta,[2] and Rainer Heintzmann[3,4,5]

Research Article Vol. 34, No. 8 / August 2017 / Journal of the Optical Society of America A 1339

Journal of the Optical Society of America A

OPTICS, IMAGE SCIENCE, AND VISION

Image formation in image scanning microscopy, including the case of two-photon excitation

Colin J. R. Sheppard,[1,*] Marco Castello,[1,2] Giorgio Tortarolo,[1,2] Giuseppe Vicidomini,[1] and Alberto Diaspro[1,2,3]

With Stokes shift, large array

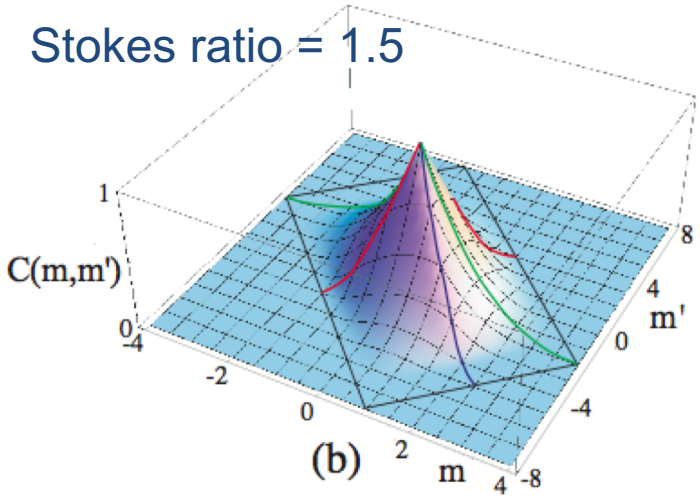

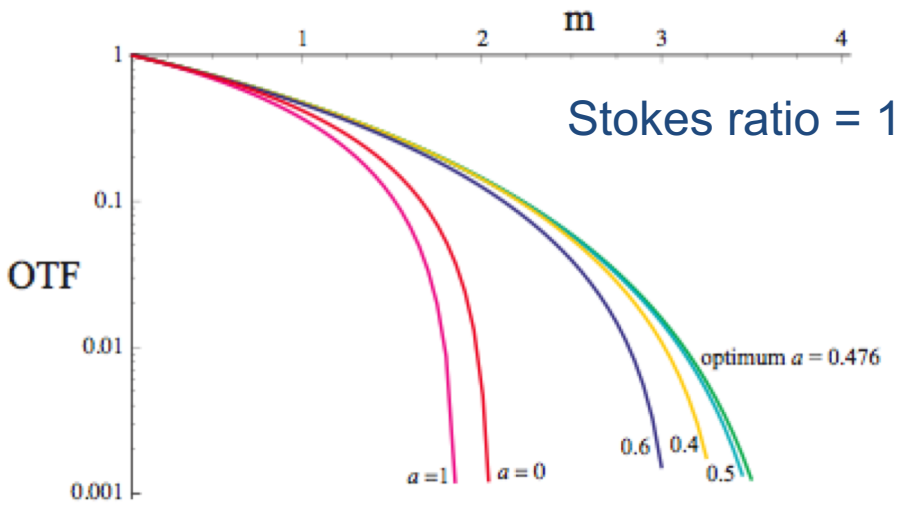

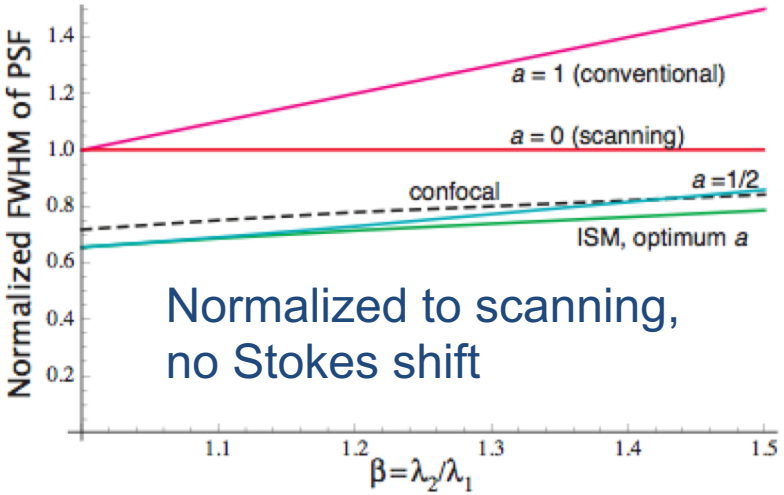

Fig.6. The variation in the normalized FWHM of the point spread function with Stokes shift ratio, for different values of the reassignment factor a , for ISM with a large detector array.

- scanning is better than conventional
- true confocal is better
- ISM for optimum *a* is even better
- ISM for *a*=1/2 is better than confocal for Stokes ratio<1.4
- *a*=1/2 is OK for Stokes ratio of 1.1

Research Article Vol. 34, No. 8 / August 2017 / Journal of the Optical Society of America A 1339

Journal of the Optical Society of America A
OPTICS, IMAGE SCIENCE, AND VISION

Image formation in image scanning microscopy, including the case of two-photon excitation

COLIN J. R. SHEPPARD,[1,*] MARCO CASTELLO,[1,2] GIORGIO TORTAROLO,[1,2] GIUSEPPE VICIDOMINI,[1] AND ALBERTO DIASPRO[1,2,3]

Circular detector array

Can use different reassignment factors *a* for different detector offsets

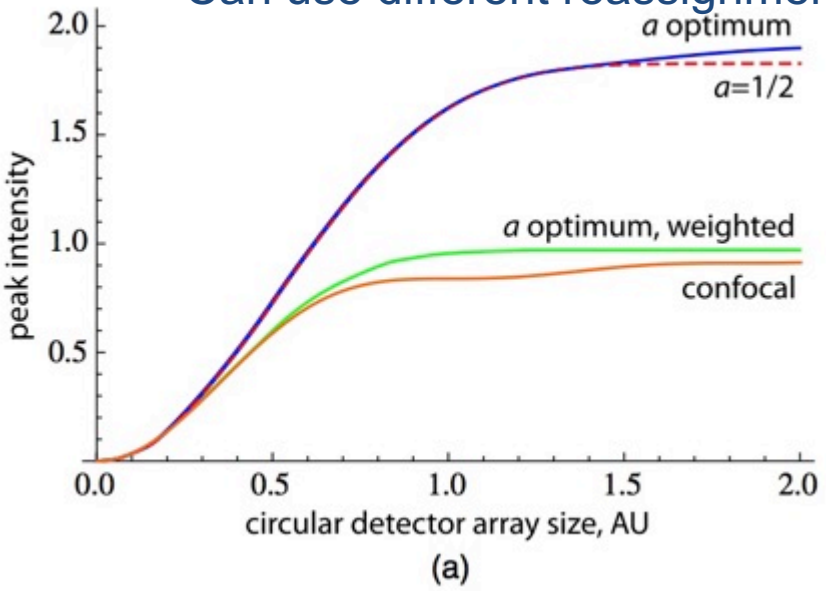

Optimum value of *a*

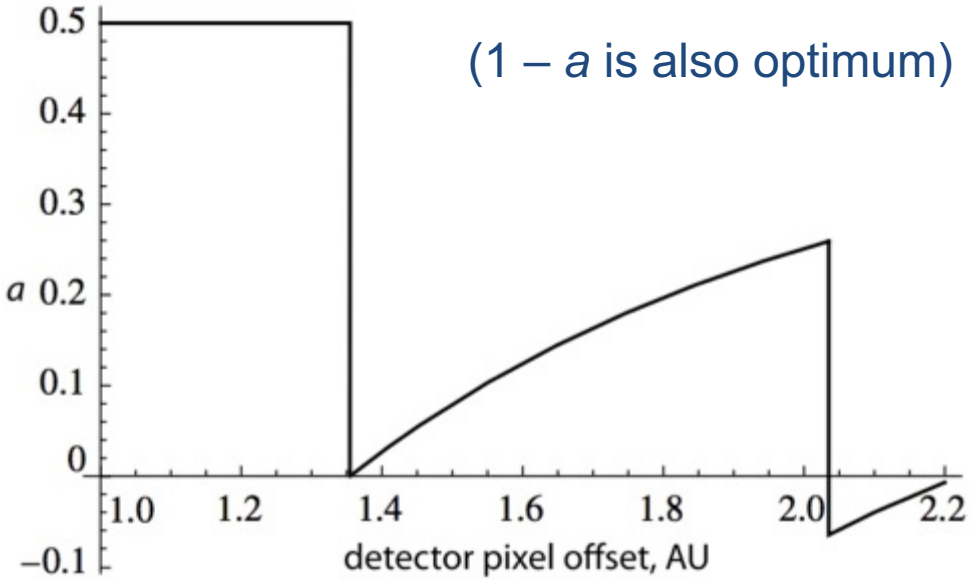

(1 – *a* is also optimum)

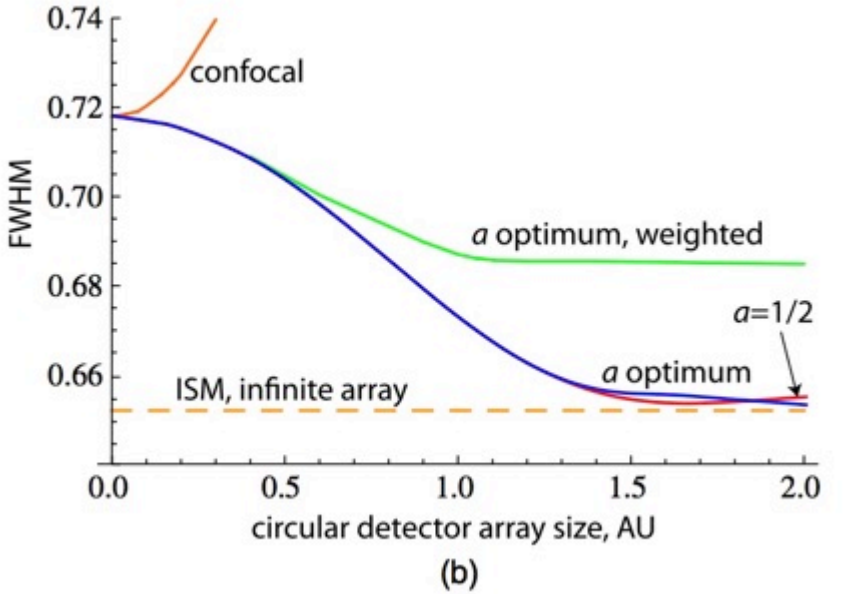

Optimum *a* gives maximum possible signal for a thin object;
most likely origin of a photon
'Weighted' means by strength of peak


154 Vol. 37, No. 1 / January 2020 / Journal of the Optical Society of America A Research Article

Journal of the Optical Society of America A
OPTICS, IMAGE SCIENCE, AND VISION

Pixel reassignment in image scanning microscopy: a re-evaluation

COLIN J. R. SHEPPARD,[1,2,*] MARCO CASTELLO,[3] GIORGIO TORTAROLO,[3,4] TAKAHIRO DEGUCHI,[1] SAMI V. KOHO,[3] GIUSEPPE VICIDOMINI,[3] AND ALBERTO DIASPRO[1,5]

Axial PSF

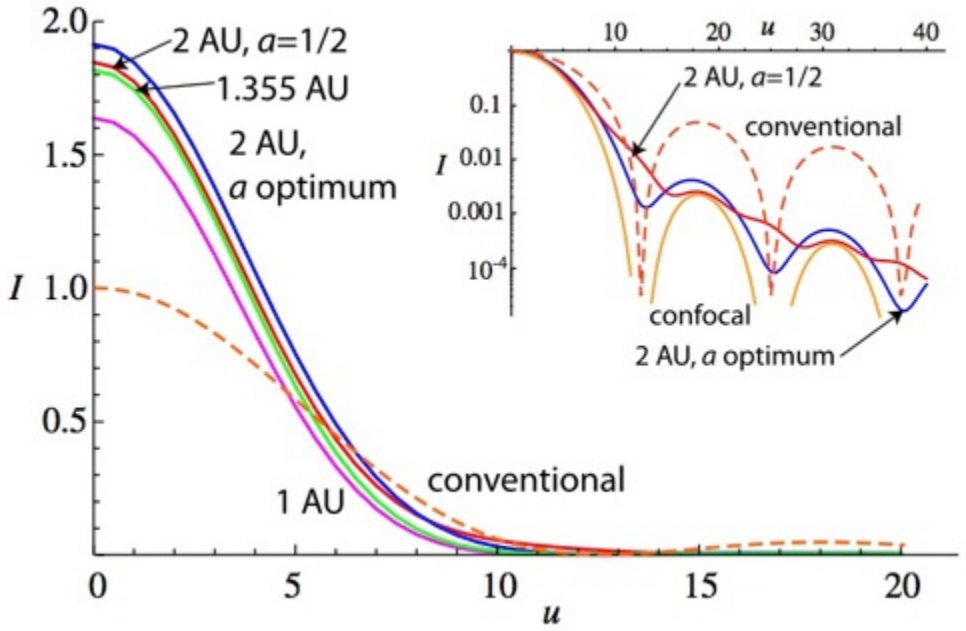

Axial PSF

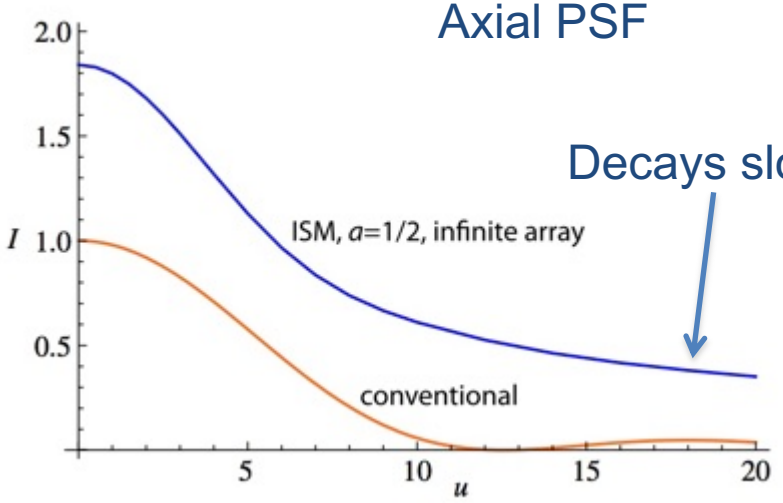

Decays slowly

Axial PSF for large array

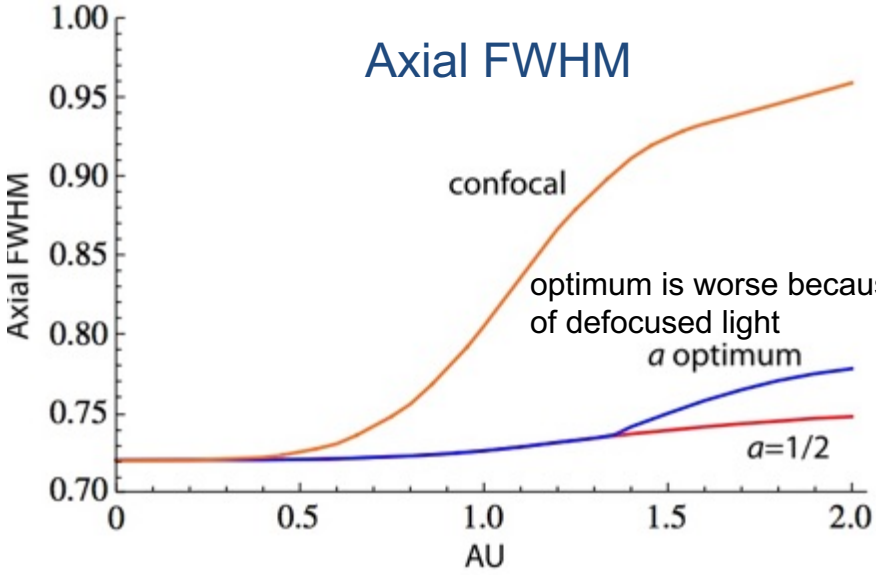

The FWHM of the axial PSF, normalized to unity for a conventional microscope. The FWHM for ISM remains almost independent of detector array size up to a size of 1.355 AU.


154 Vol. 37, No. 1 / January 2020 / Journal of the Optical Society of America A Research Article

Journal of the Optical Society of America A

OPTICS, IMAGE SCIENCE, AND VISION

Pixel reassignment in image scanning microscopy: a re-evaluation

COLIN J. R. SHEPPARD,[1,2,*] MARCO CASTELLO,[3] GIORGIO TORTAROLO,[3,4] TAKAHIRO DEGUCHI,[1] SAMI V. KOHO,[3] GIUSEPPE VICIDOMINI,[3] AND ALBERTO DIASPRO[1,5]

Two-photon fluorescence ISM

Large array

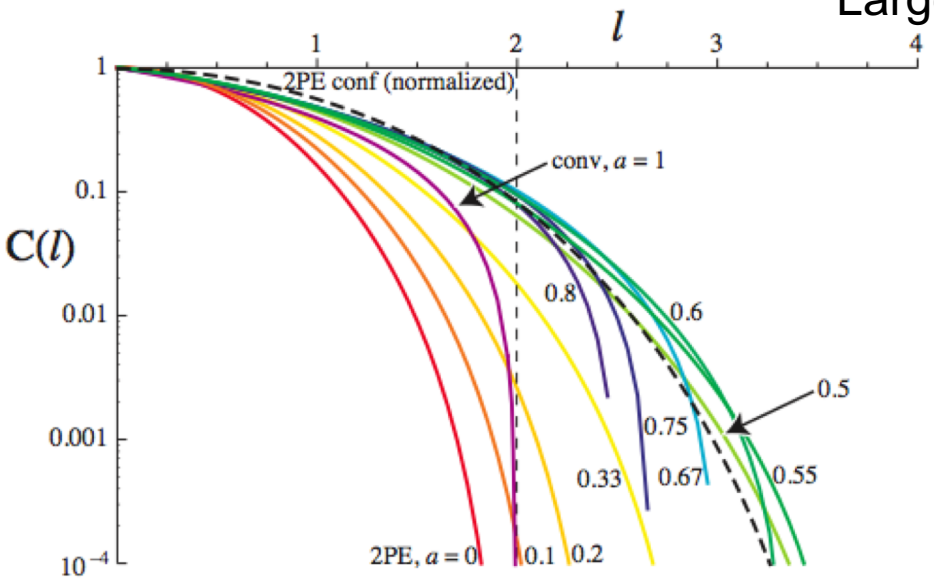

Fig. 1. The OTF for two-photon fluorescence with different reassignment factors, a. A value of zero gives a 2PE fluorescence microscopy with a large detector. A value of unity gives an image identical to that in a conventional 1PE fluorescence microscope. The

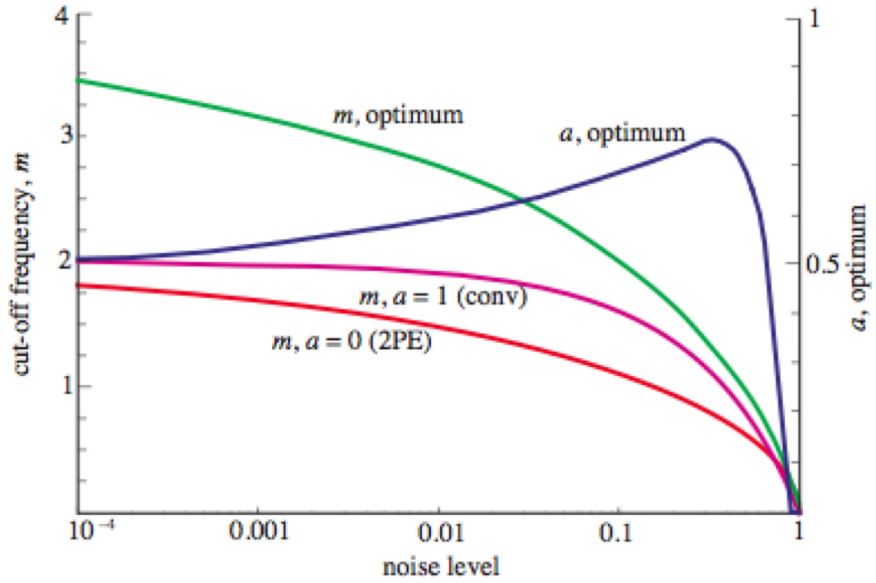

Fig.2. The useful cut-off frequency m, as a function of the noise level, for pixel reassignment with the optimum value of reassignment factor a (green curve). The optimum value of a is also shown (blue curve). The useful cut-off frequencies for conventional 1PE and 2PE are shown for comparison (purple and red curves, respectively).

- Can alter reassignment factor *a* with spatial frequency
- OTF is

$$C_{\text{eff}}(l) = C_1[(1-a)l]C_2(al).$$

  - Resolution improved compared with two-photon fluorescence with a large single-element detector

Research Article Vol. 34, No. 8 / August 2017 / Journal of the Optical Society of America A 1339

Journal of the Optical Society of America A

OPTICS, IMAGE SCIENCE, AND VISION

Image formation in image scanning microscopy, including the case of two-photon excitation

Colin J. R. Sheppard,[1,*] Marco Castello,[1,2] Giorgio Tortarolo,[1,2] Giuseppe Vicidomini,[1] and Alberto Diaspro[1,2,3]

ISM with Bessel beam, and 2 photon ISM

Optimum value of *a*

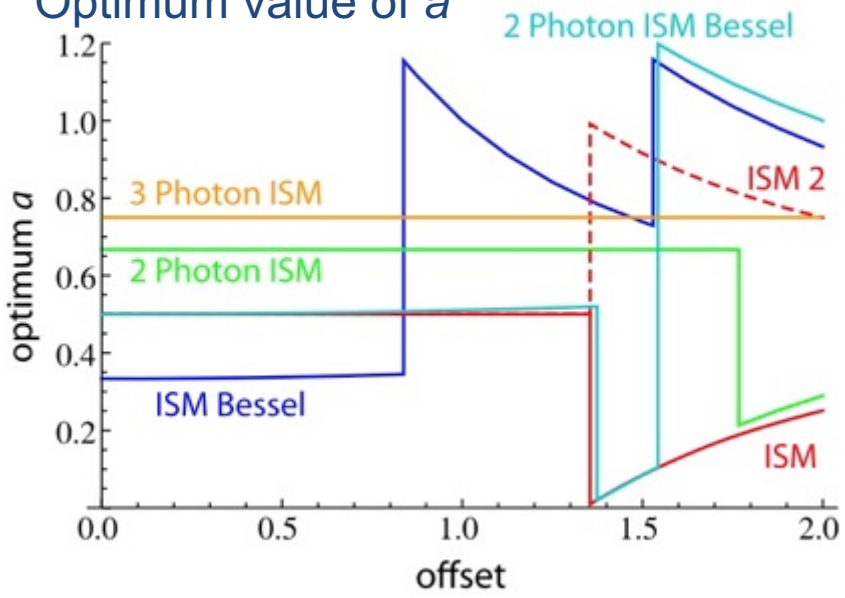

2, 3 photon are for same emission wavelength as 1 photon

FWHM

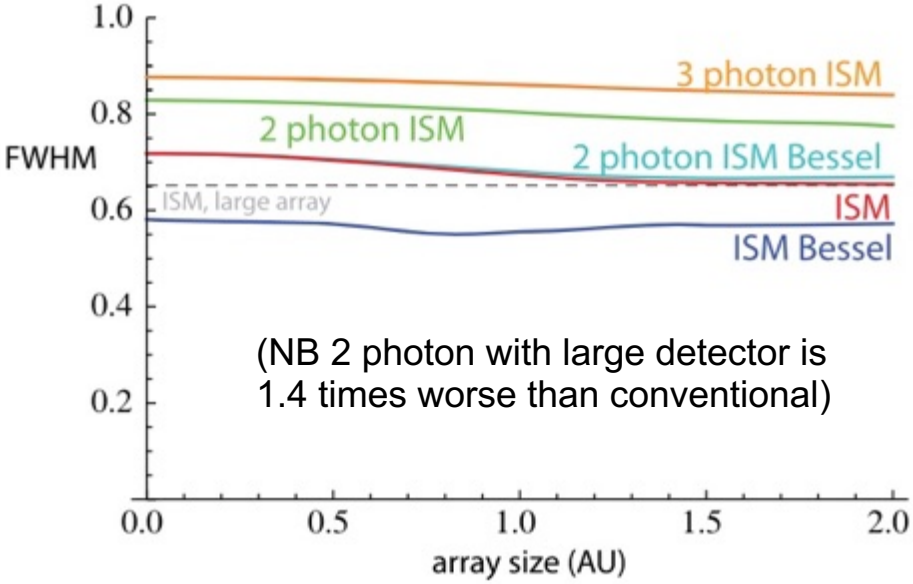

(NB 2 photon with large detector is 1.4 times worse than conventional)

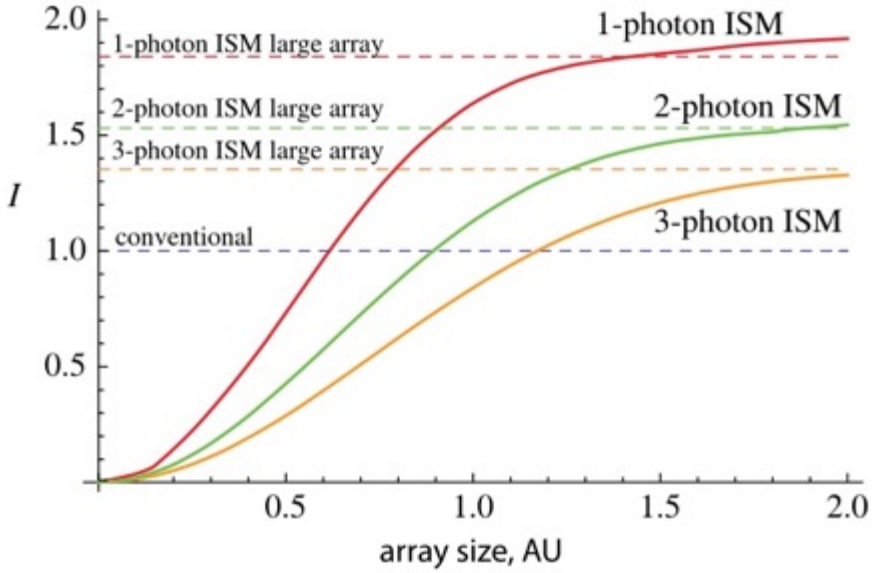

Peak intensity, normalized to conventional

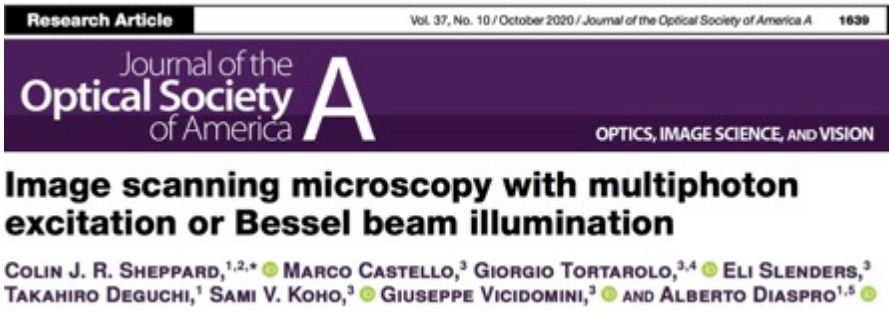

Doughnut beam excitation

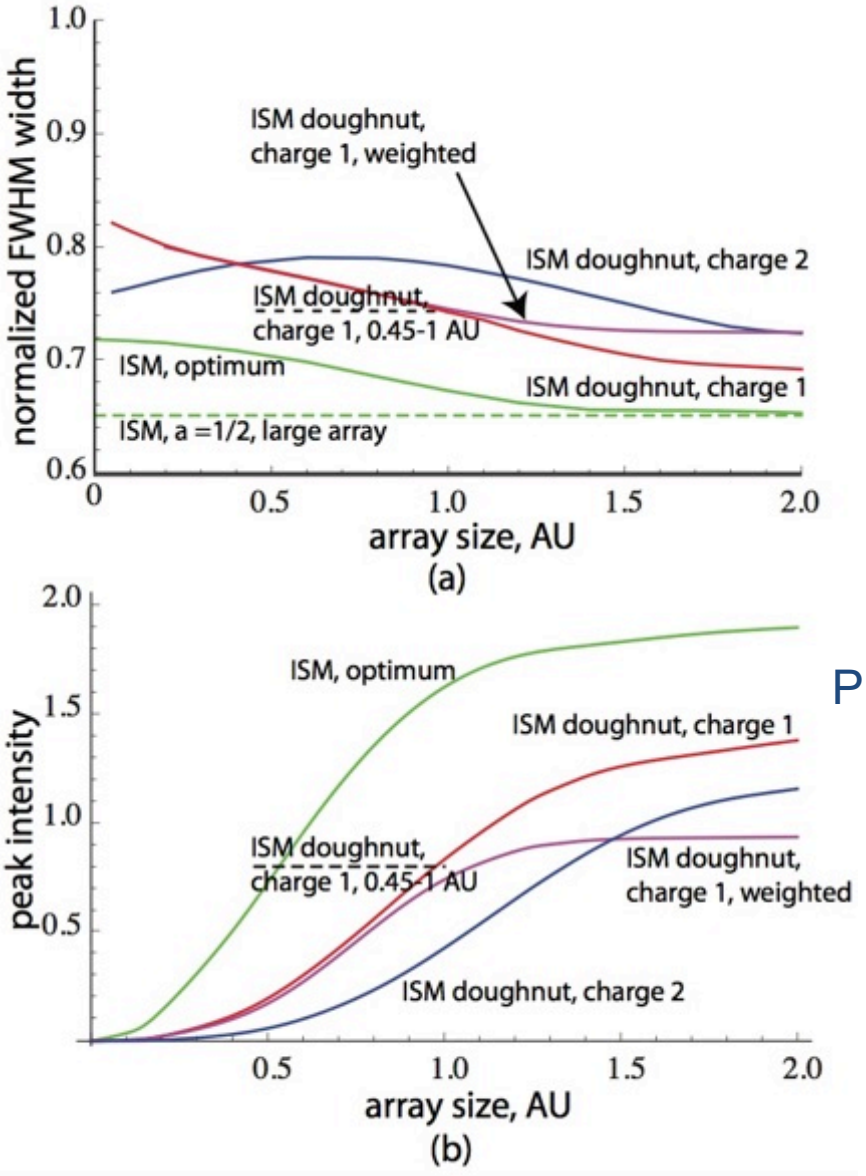

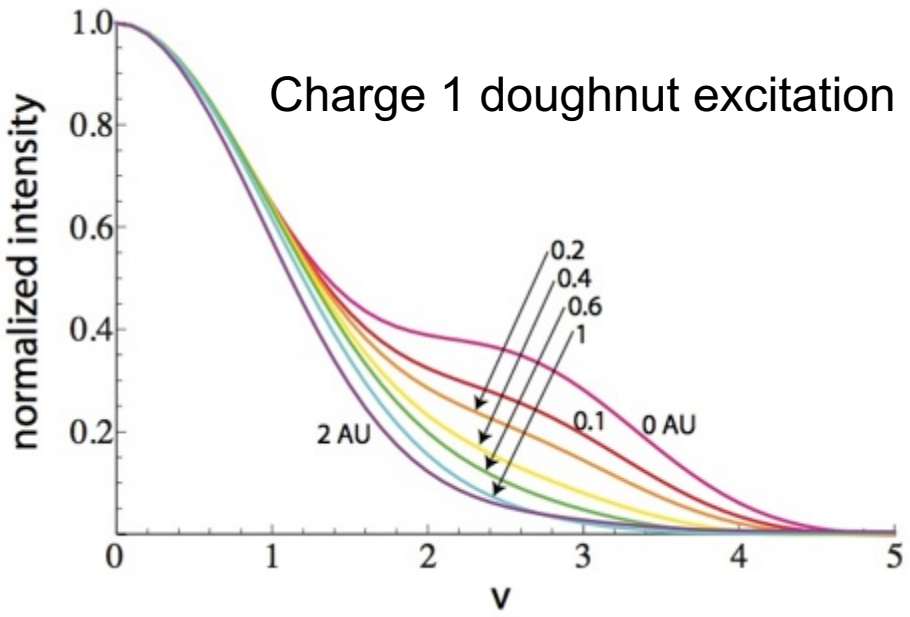

Pixel reassignment corrects for doughnut beam!

Pixel reassignment in image scanning microscopy with a doughnut beam: An example of maximum likelihood restoration

COLIN J. R. SHEPPARD[1,2,*], MARCO CASTELLO[3], GIORGIO TORTAROLO[3,4], ELI SLENDERS[3], TAKAHIRO DEGUCHI[1], SAMI V. KOHO[3], PAOLO BIANCHINI[1], GIUSEPPE VICIDOMINI[3], AND ALBERTO DIASPRO[1,5]

J. Opt. Soc. Am A **38**, 1075-1084 (2021).

Axial PSF

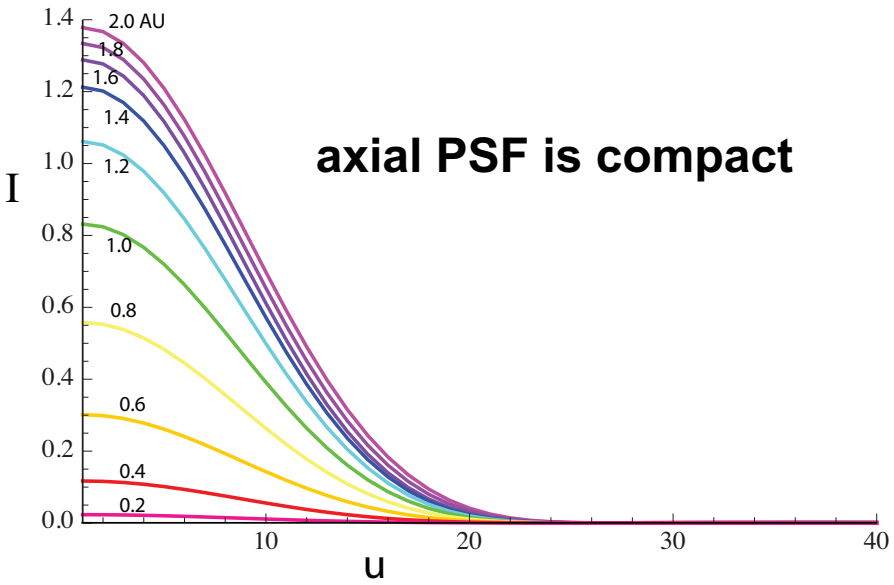

normalized axial distance

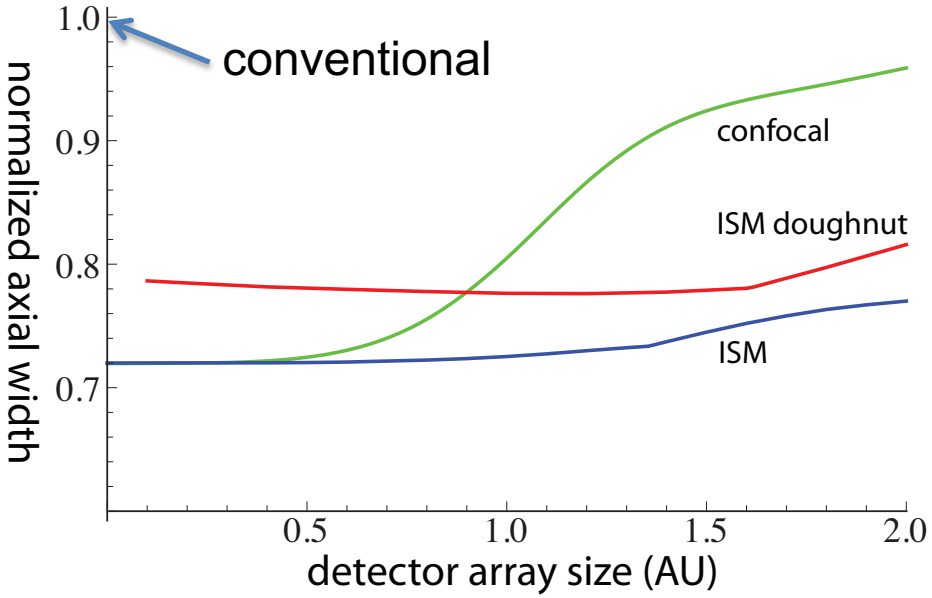

The axial cross-section through the PSF for dISM with a circular disk-shaped detector array and charge 1 doughnut beam illumination, after reassignment.

The axial resolution (width of the axial cross-section through the PSF, normalized to unity for conventional imaging) for dISM with a circular disk-shaped detector array and charge 1 doughnut beam illumination, after reassignment. The behavior for ISM, and for confocal microscopy with a pinhole of the same size as the array are also shown.

Integrated intensity:
A measure of optical sectioning

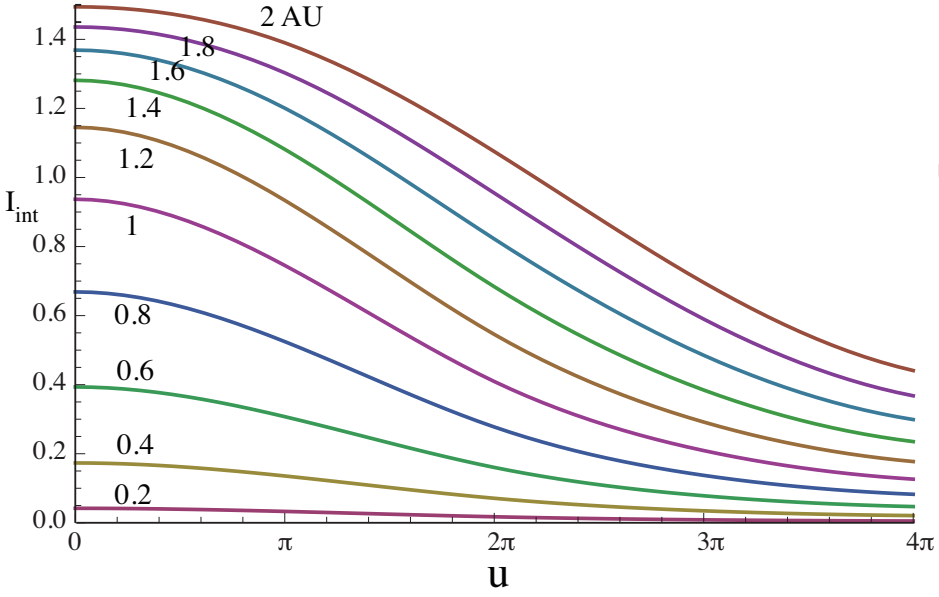

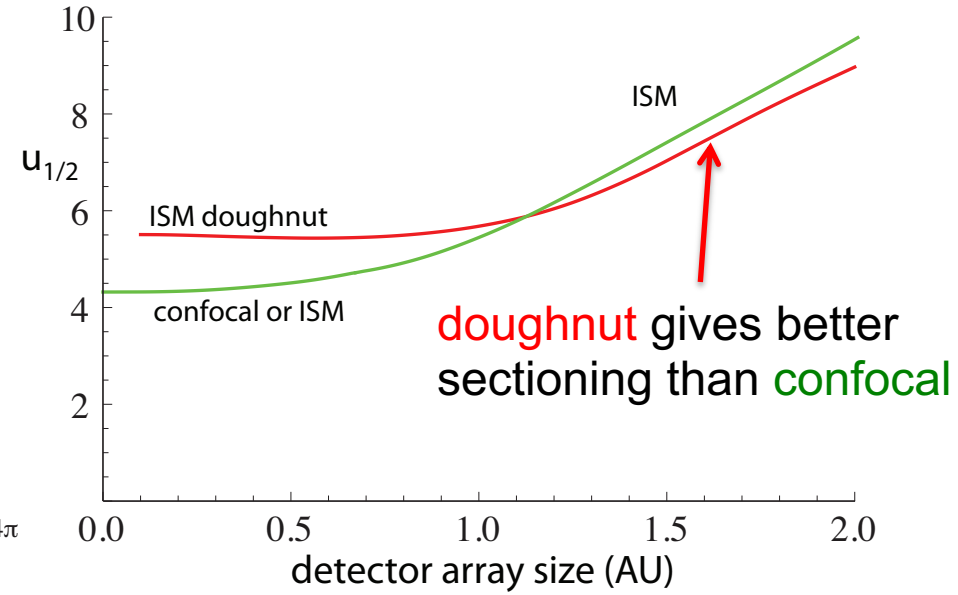

The variation in integrated intensity with defocus for dISM with charge 1 doughnut illumination. Curves are plotted for array sizes from 0.2 AU to 2 AU insteps of 0.2 AU.

The axial distance $u_{1/2}$ for the integrated intensity to fall to half the in-focus value, as a function of detector array size, for dISM with charge 1 doughnut illumination or with Airy disk illumination. The behavior for confocal microscopy with a pinhole of the same size as the array is also shown.

Cross-sections through PSF for offset point detector

Offset in *x*. Maximum intensity always lies in *x*-*z* plane.

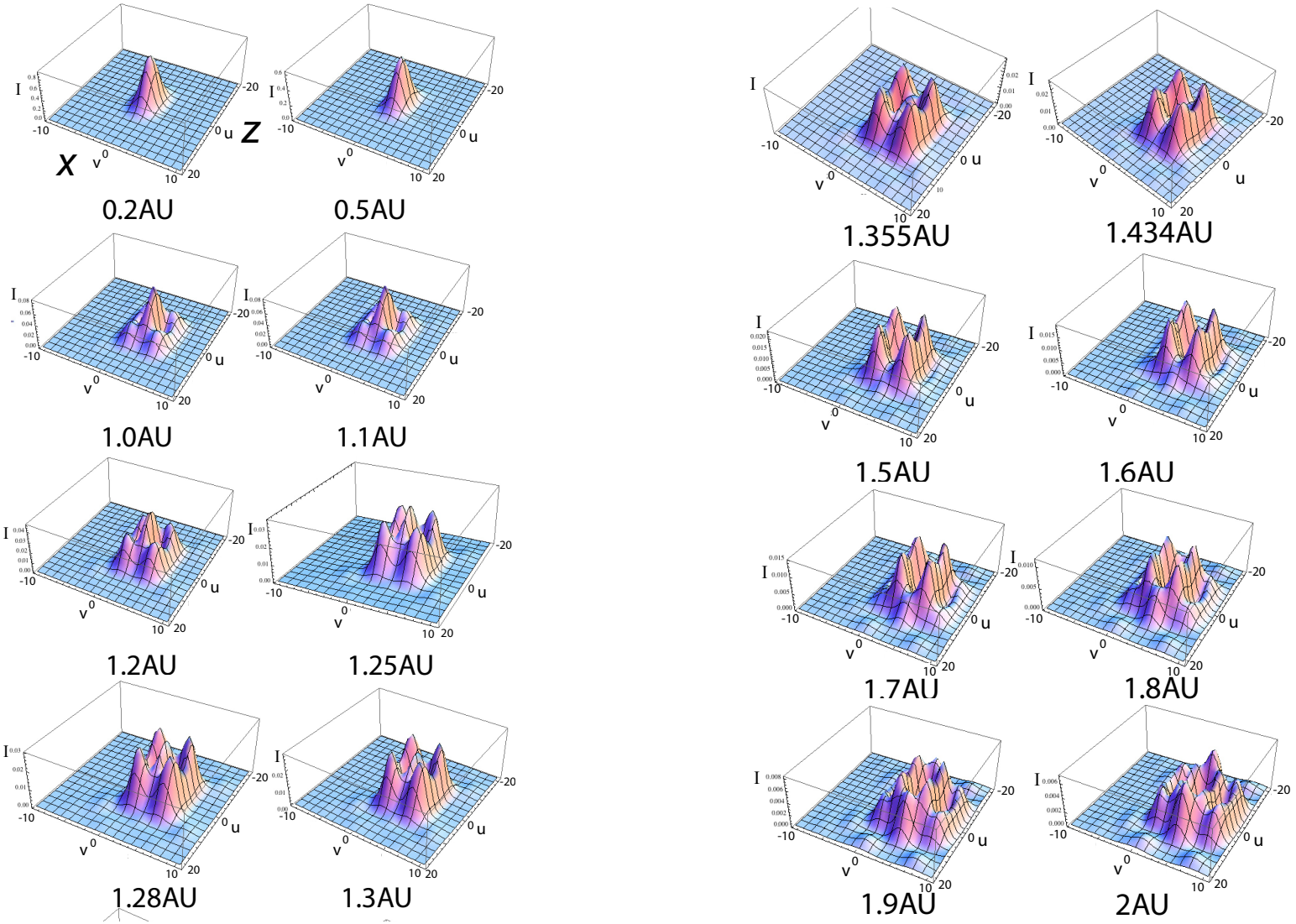

Signal from offset detector

- v_d=4.9046, 1.28AU, 5 equal peaks in *x*-*z* plane
- v_d=5.192, 1.355AU, 3 equal peaks in *x* for *z*=0
- v_d=5.494, 1.434AU, leaves focal plane, $I(z)$ is flat

Pixel reassignment factor, *a*

Reassignment to bring different peaks to centre

Larger offset can give information from defocused parts of object

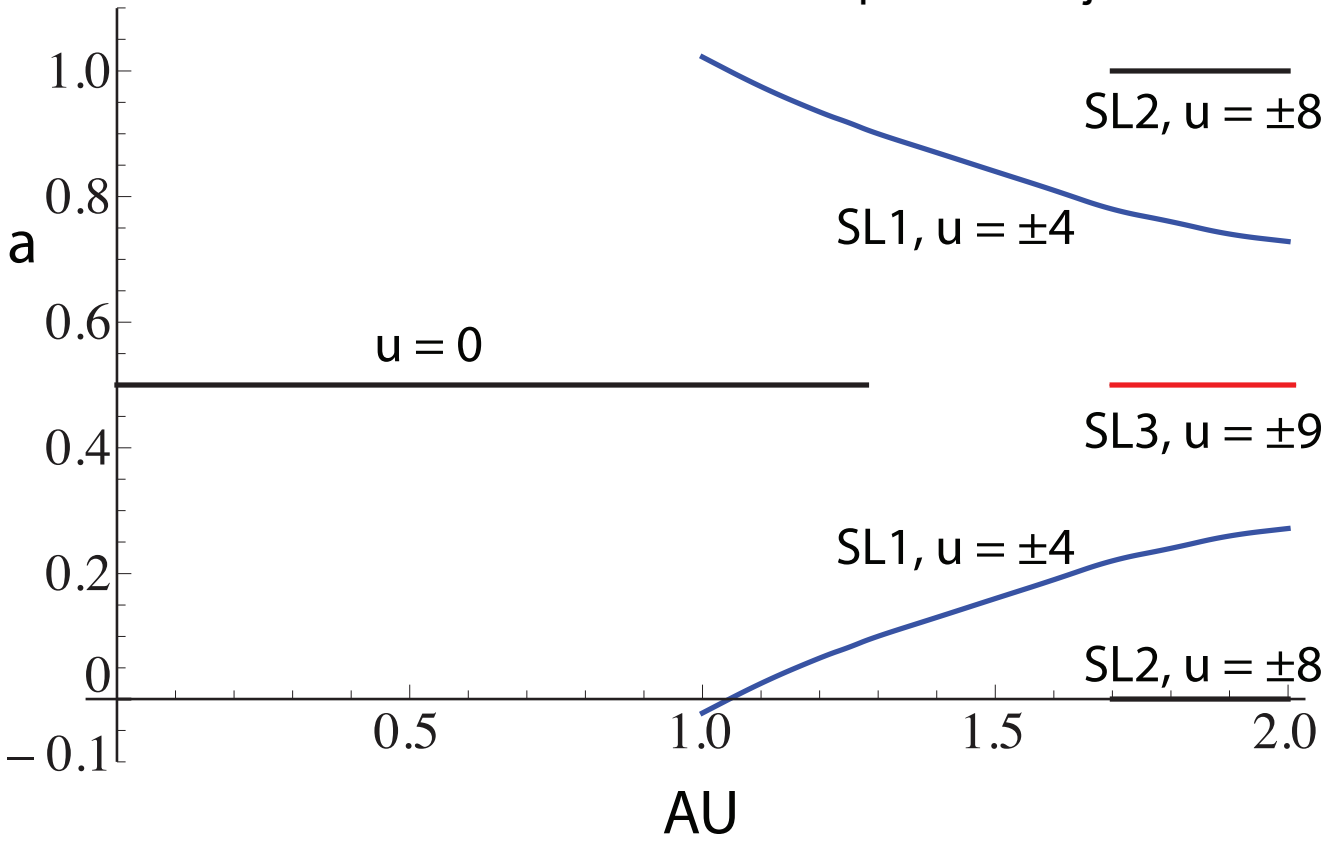

Signal from centrally illuminated point object

The intensity in the plane of the detector for a centrally illuminated point object is $I_{\text{point}}(V) = H_2(v)$. The signal S_{point} from a centrally illuminated point object with a pinhole of radius v_d is

$$S_{\text{point}}(v_d) = 1 - J_0^2(v_d) - J_1^2(v_d). \quad \textbf{(3)}$$

(Well known result. In e.g. Born & Wolf)

Fluorescent sheet, or integrated intensity

The intensity in the plane of the detector for a fluorescent sheet is

$$\begin{aligned} I_{\text{sheet}}(v) &= \text{const.} \times H_1(v) \otimes_2 H_2(v) \\ &= \text{const.} \times \int_0^2 C_{2D}^2(l) J_0(lv) l \, \mathrm{d}l \\ &= \frac{24}{3\pi^2 - 16} \int_0^2 \left[\arccos\left(\frac{l}{2}\right) - \frac{l}{2}\sqrt{1 - \frac{l^2}{4}} \right]^2 J_0(lv) l \, \mathrm{d}l, \end{aligned} \tag{4}$$

(In-focus case)

where $\otimes_{2D}$ is a 2D convolution, and $I_{\text{sheet}}(0) = 1$. The background from a fluorescent sheet, or the integrated intensity from a point object, with a pinhole of radius v_d is

$$S_{\text{sheet}}(v) = 0.405\, v_d \int_0^2 \left[\arccos\left(\frac{l}{2}\right) - \frac{l}{2}\sqrt{1 - \frac{l^2}{4}} \right]^2 J_1(l v_d) \, \mathrm{d}l, \tag{5}$$

where it is normalized to unity for large v_d.

Volume object

The 3D OTF is

$$C_{3D}(l,s) = \frac{1}{l}\sqrt{1-\left(\frac{l}{2}+\frac{|s|}{l}\right)^2}. \quad (6)$$

Then the projection along s of the square of the 3D OTF is

$$F(l) = 2\int_0^{l(1-l/2)} C_{3D}^2(l,s)\,\mathrm{d}s = \frac{(2-l)^2(4+l)}{12l}. \quad (7)$$

The intensity in the detector plane for a featureless fluorescent volume is

$$\begin{aligned} I_{\mathrm{vol}}(v) &= \int_0^2 F(l)J_0(vl)\,\mathrm{d}l \\ &= J_0(2v) - \tfrac{4}{3}J_2(2v) - \tfrac{1}{9}J_4(2v) \\ &\quad + \tfrac{4}{3}\pi\left[J_1(2v)\mathbf{H}_0(2v) - J_0(2v)\mathbf{H}_1(2v)\right], \end{aligned} \quad (8)$$

where $\mathbf{H}_n$ is a Struve function of order n. $I(0) = 1$, and for large v, $I \to 4/3v$.

The background from a featureless volume object is obtained by integrating over the pinhole, radius v_d, so that

$$\begin{aligned} B_{\mathrm{vol}} &= v_d \int_0^2 C_{3D}^2 J_1(v_d l)\,\mathrm{d}l \\ &= (\tfrac{3}{4}+v_d^2)J_0(2v_d) + (\tfrac{1}{4}-v_d^2)J_2(2v_d) - \tfrac{3}{4} \\ &\quad + \pi v_d^2\left[J_1(2v)\mathbf{H}_0(2v) - J_0(2v)\mathbf{H}_1(2v)\right], \end{aligned} \quad (9)$$

where it has been renormalized so that a good approximation for $v_d > 1.5$, is that $B_{\mathrm{vol}} \approx (v_d - 3/4)$. The background increasas linearly with v_d for large pinhole sizes.

(1st part from Gu M, Sheppard, CJR (1991) Effects of finite-sized detector on the OTF of confocal fluorescent microscopy, *Optik* **89**, 65-69. 2nd part from Sheppard CJR, Gan XS, Gu M, Roy M (2007) Signal-to-Noise Ratio in Confocal Microscopes, Chapter 22 in *The Handbook of Biological Confocal Microscopy*, 3rd edition, J. Pawley, ed. Springer, New York, pp. 442-452)

(New analytical result)

(New analytical result)

Intensity in detector plane

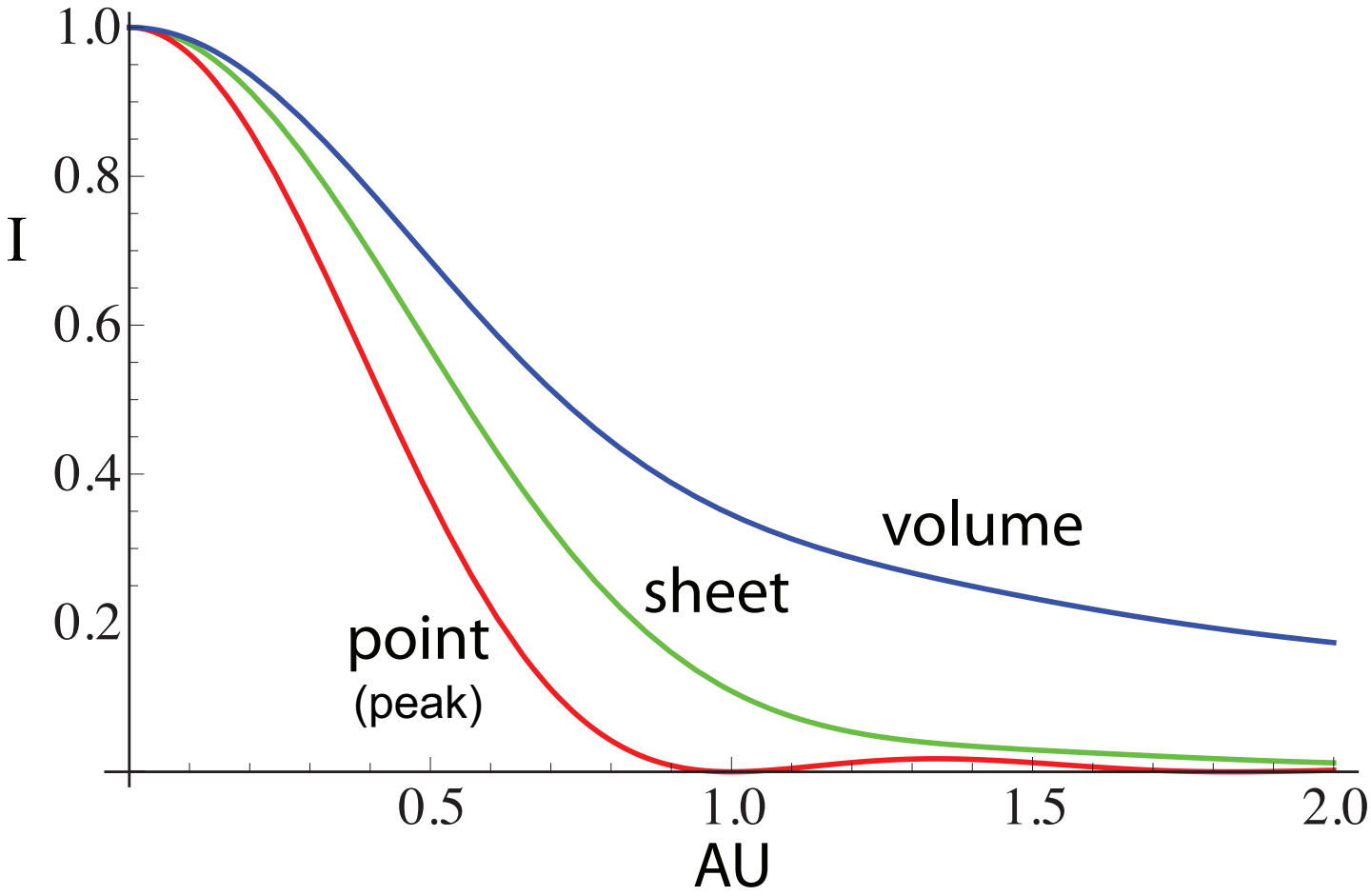

Signal from point, and integrated intensity, or background from a sheet

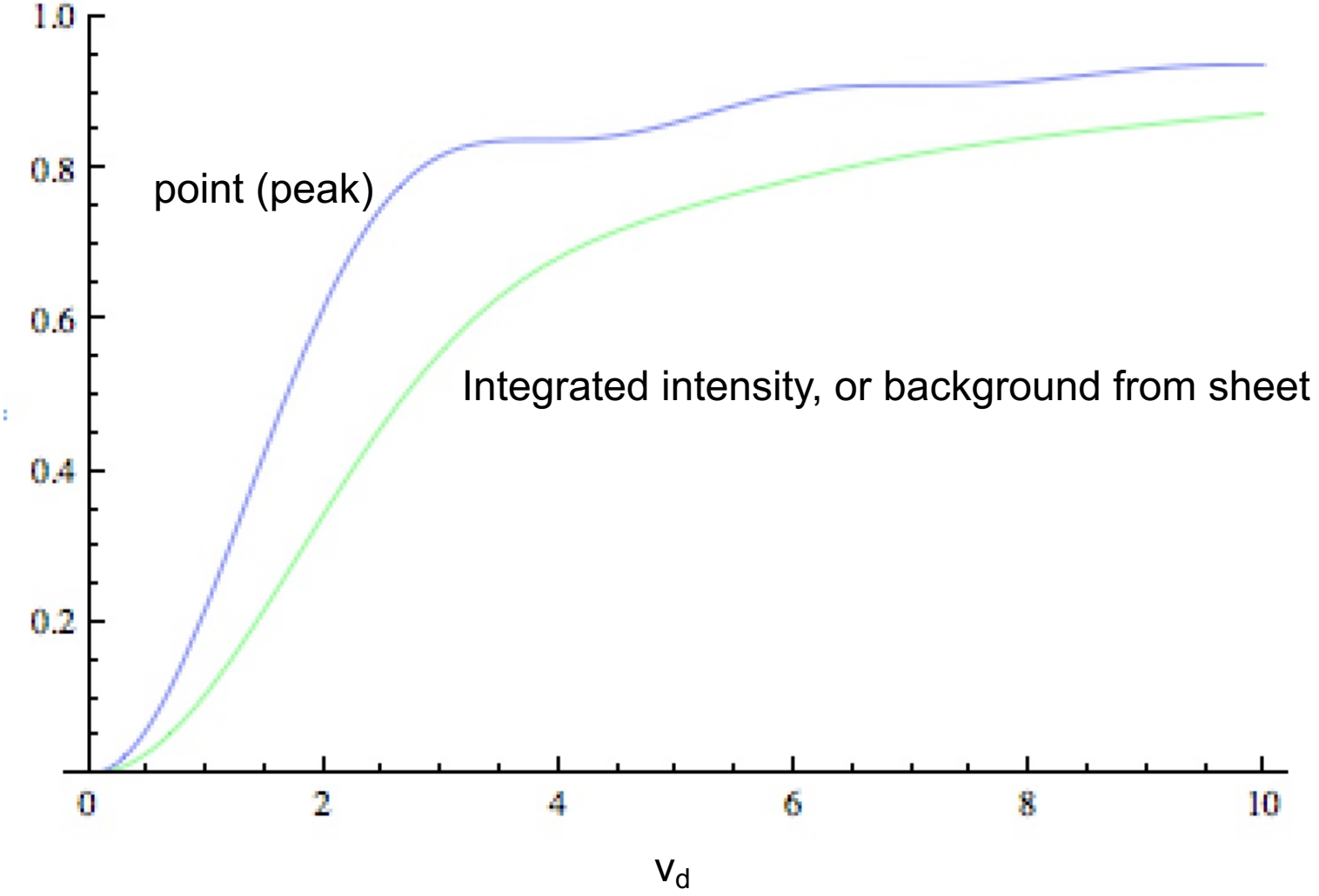

Background from volume

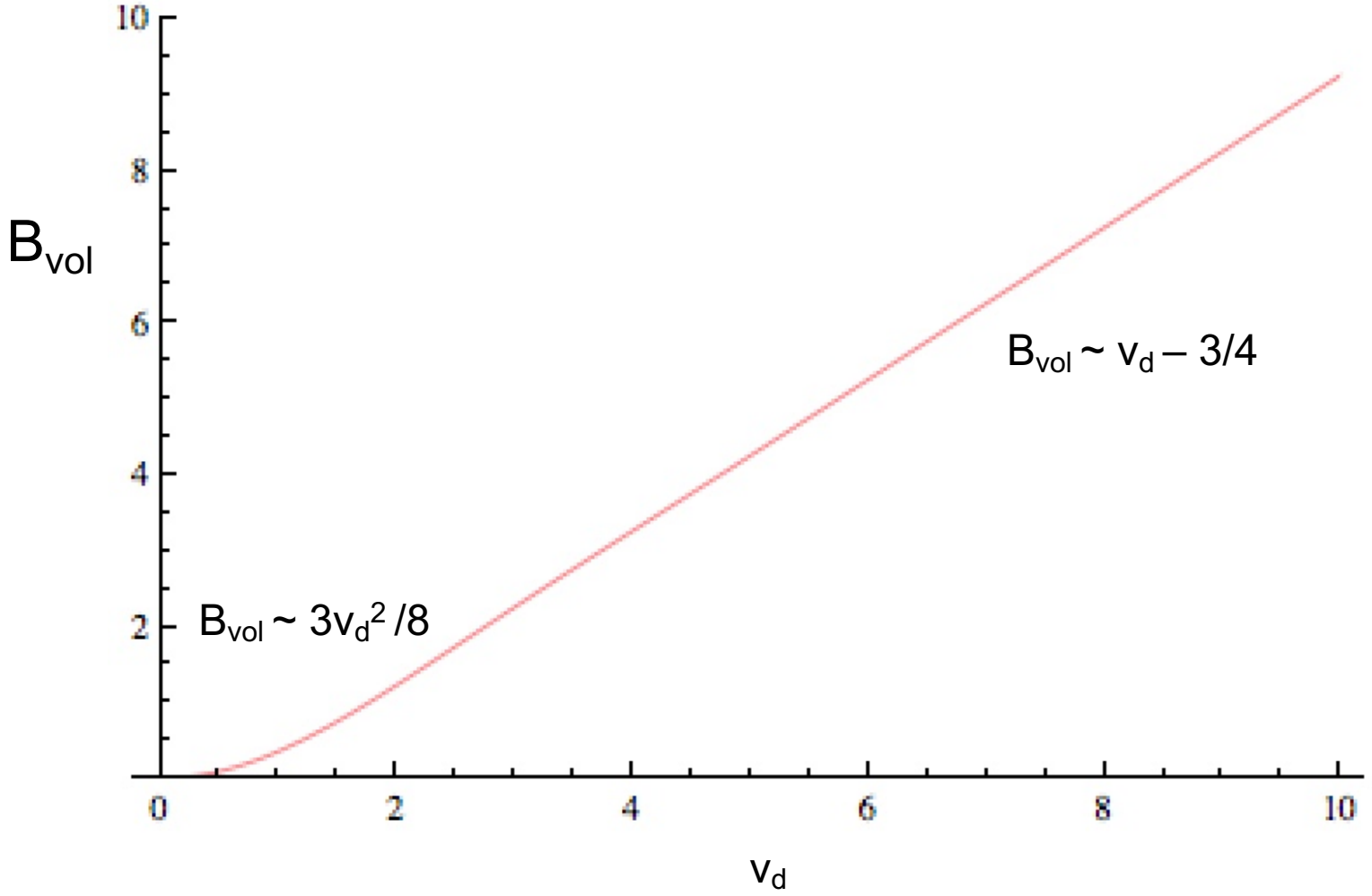

Detectability

Defined as signal / background$^{1/2}$

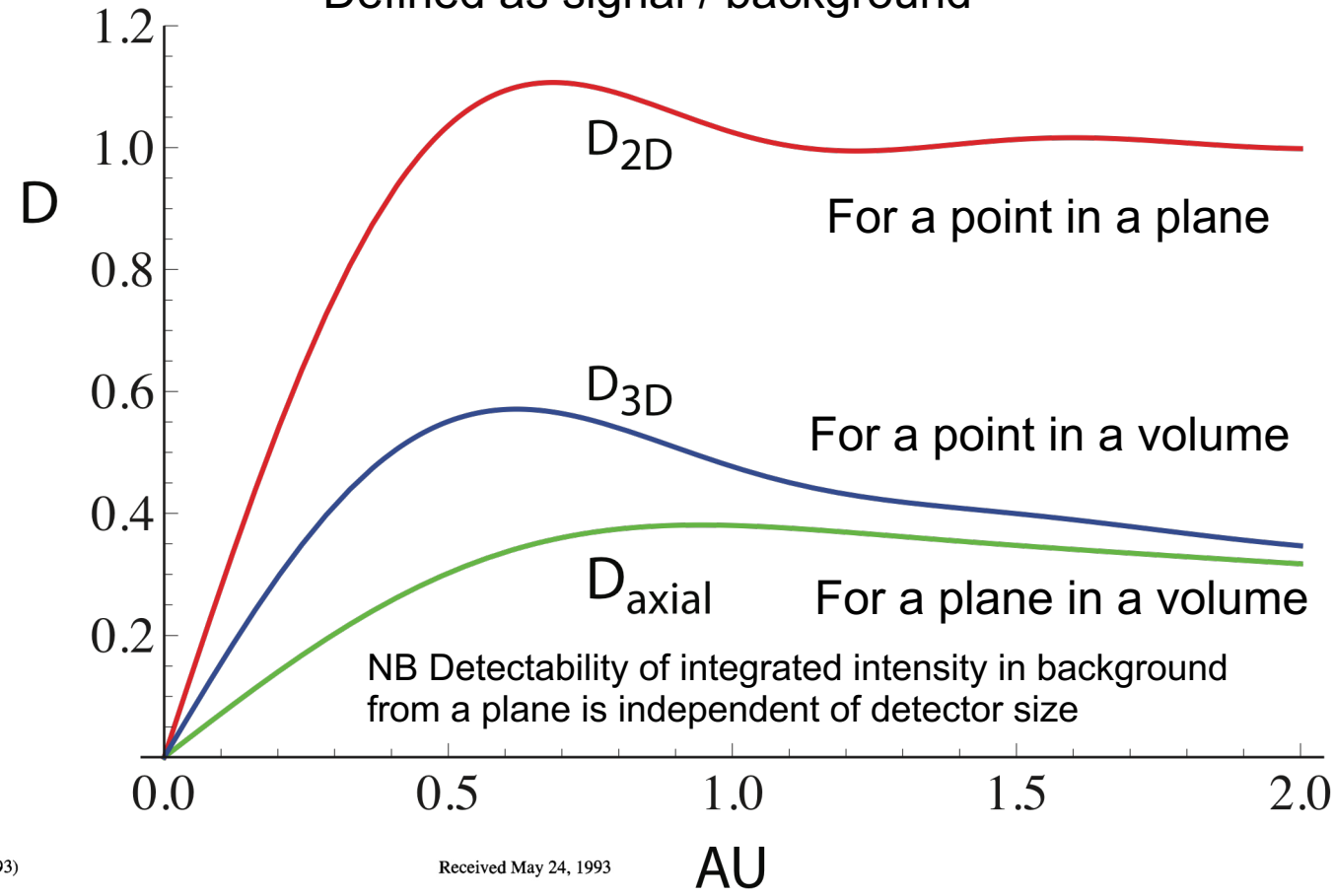

SCANNING Vol. 15, 187–192 (1993)

Received May 24, 1993

Original Papers

Detectability: A New Criterion for Evaluation of the Confocal Microscope

X.S. Gan and C.J.R. Sheppard

22

Signal-to-Noise Ratio in Confocal Microscopes

Colin J.R. Sheppard, Xiaosong Gan, Min Gu, and Maitreyee Roy

Integrated intensity from offset point detector

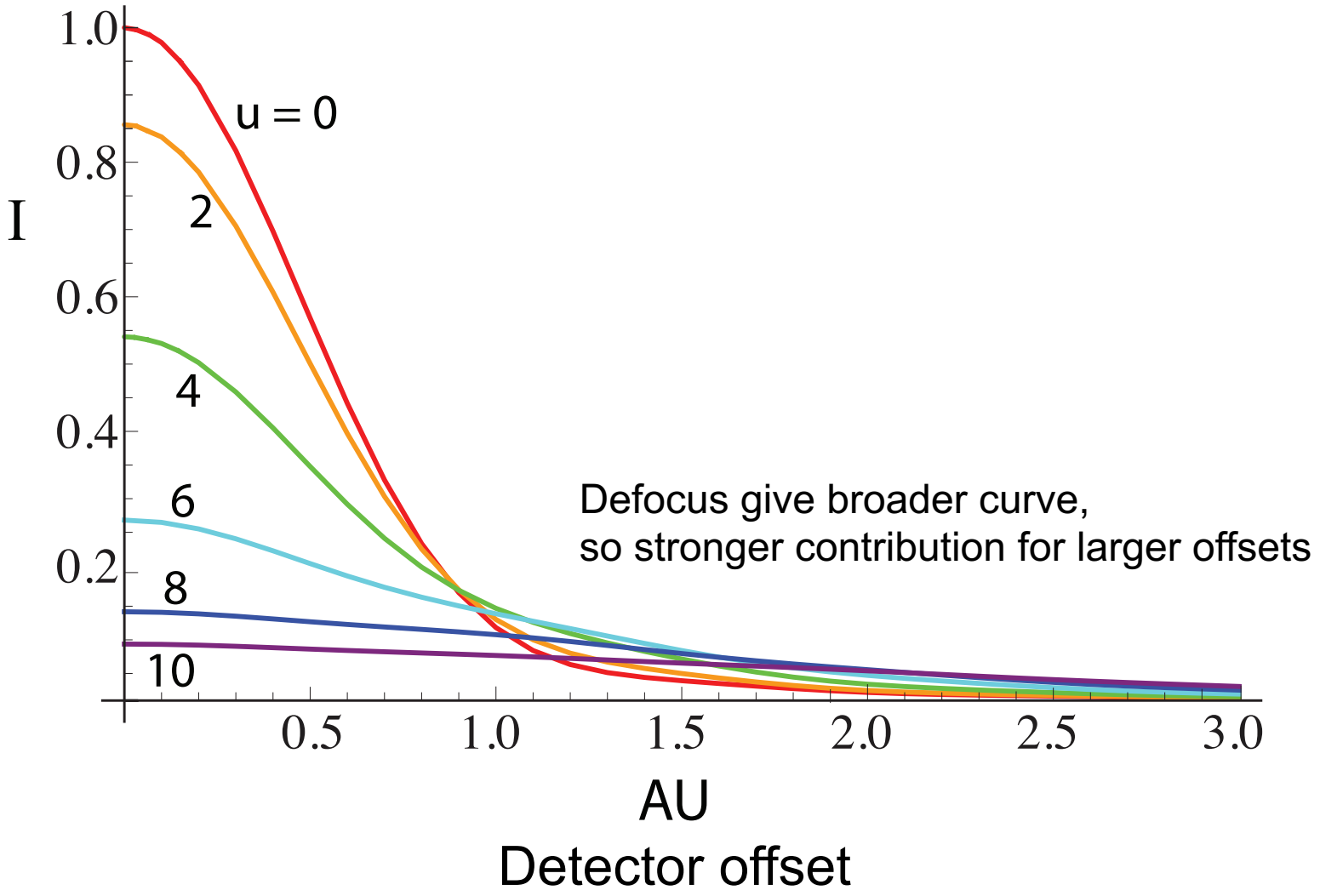

Integrated intensity from offset point detector with defocus: Fingerprint

Larger offsets give broader curve,
so stronger contribution from out-of-focus light

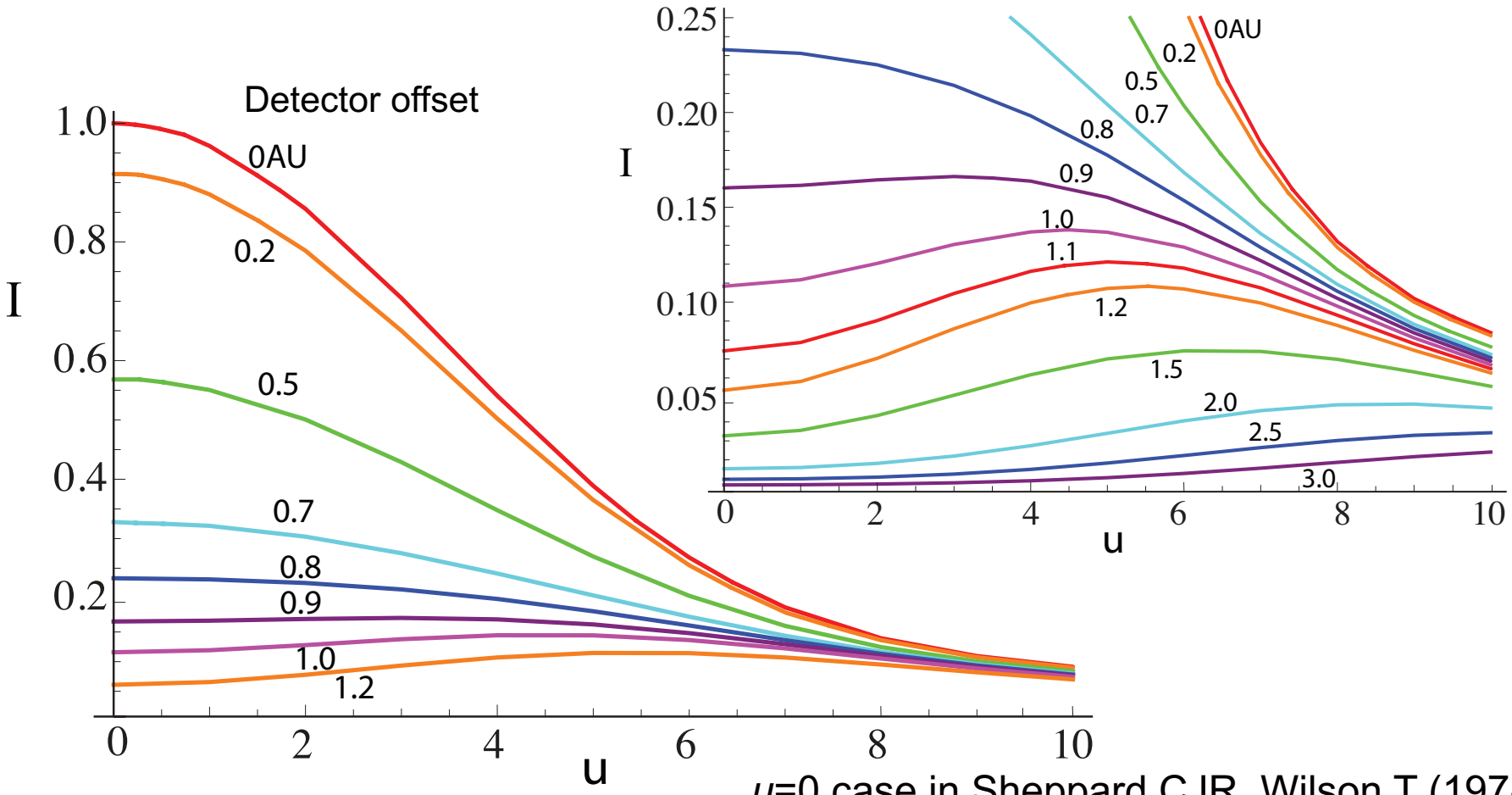

u=0 case in Sheppard CJR, Wilson T (1978) Depth of field in the scanning microscope, *Optics Letts.* **3**, 115-117.

Integrated intensity from a ring of offset point detectors

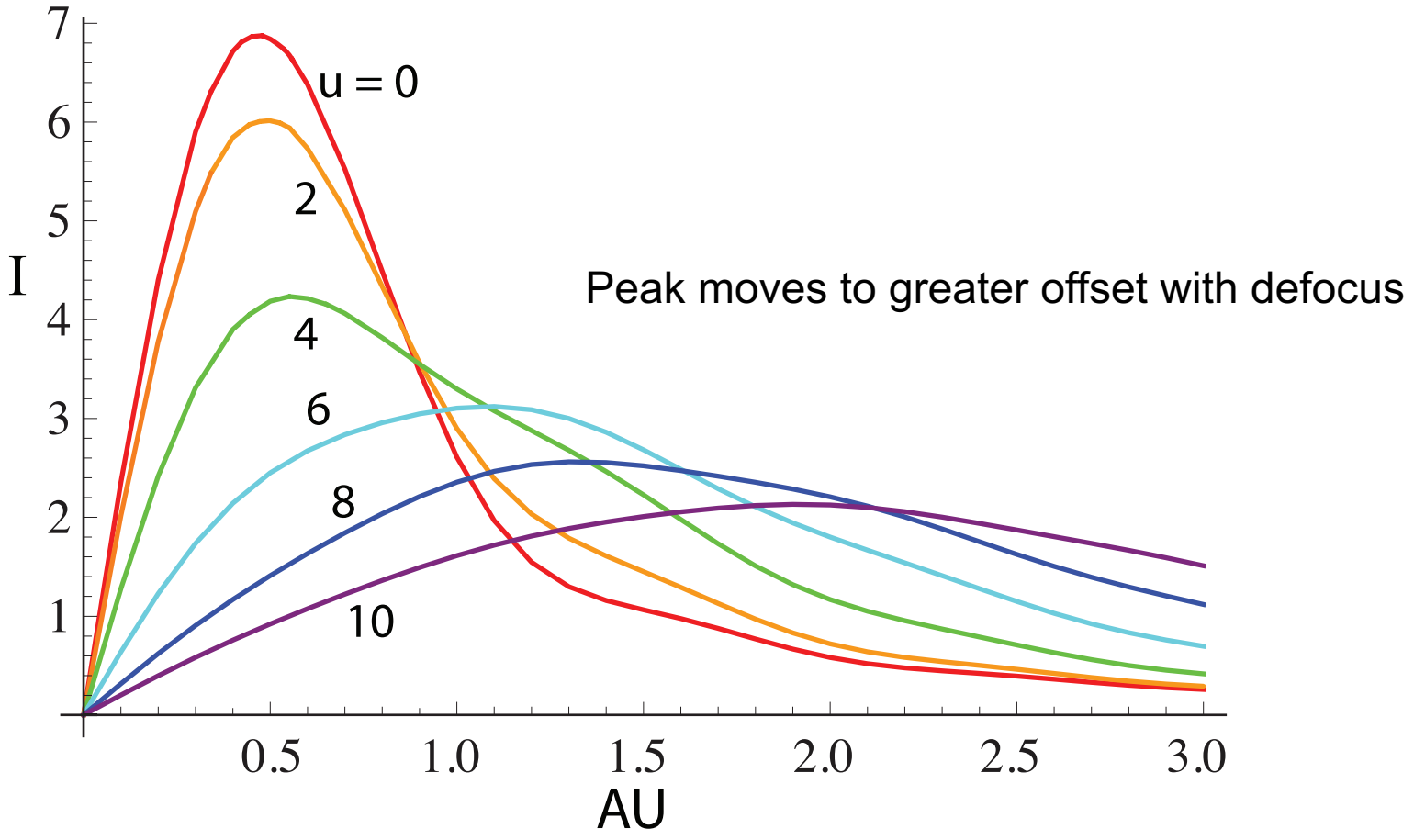

Integrated intensity from a ring of offset point detectors with defocus: Fingerprint of the ring

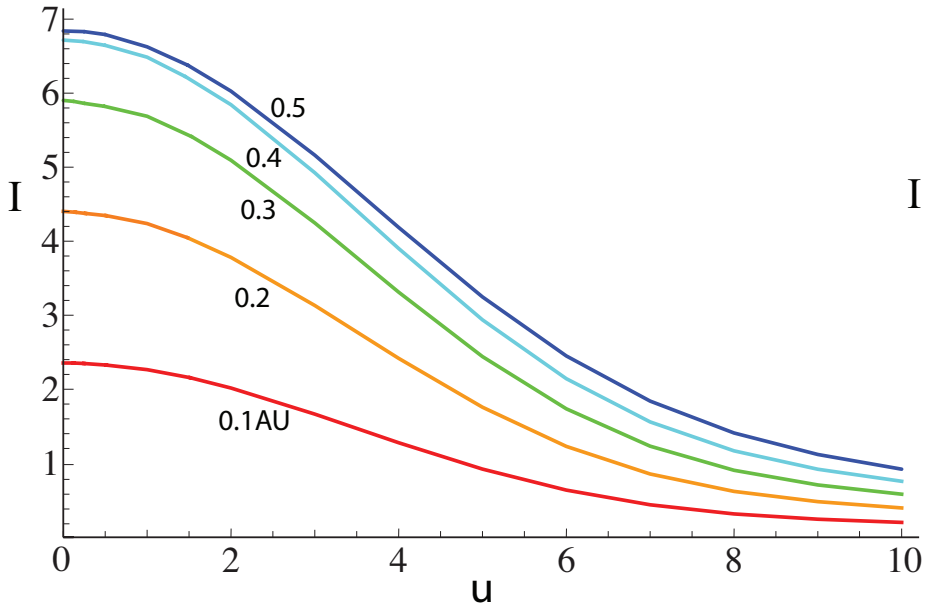

For small ring radius, signal increases with radius, but shape of curve changes little.

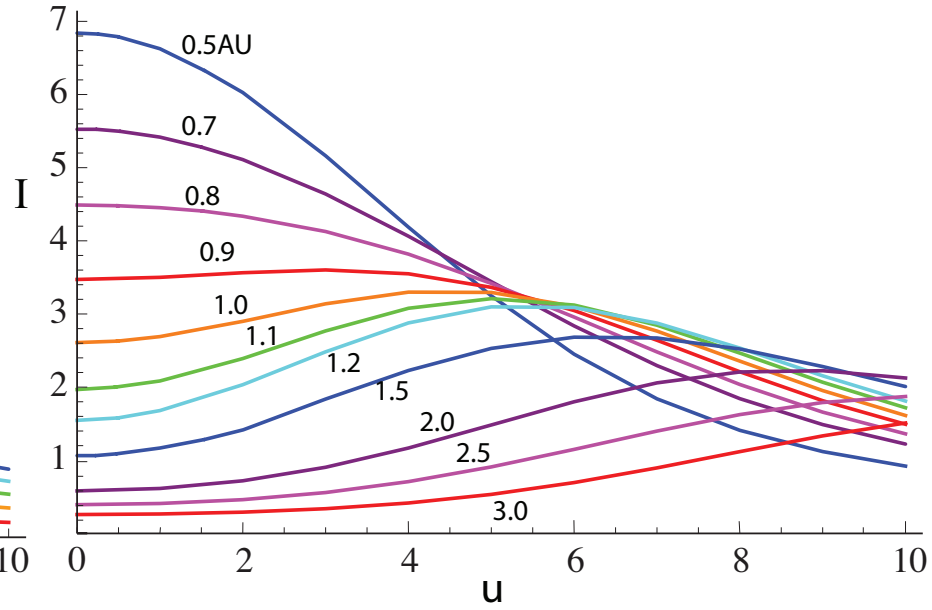

For large ring radius, peak of signal occurs for defocused sheet.

Defocused sheet with disk detector

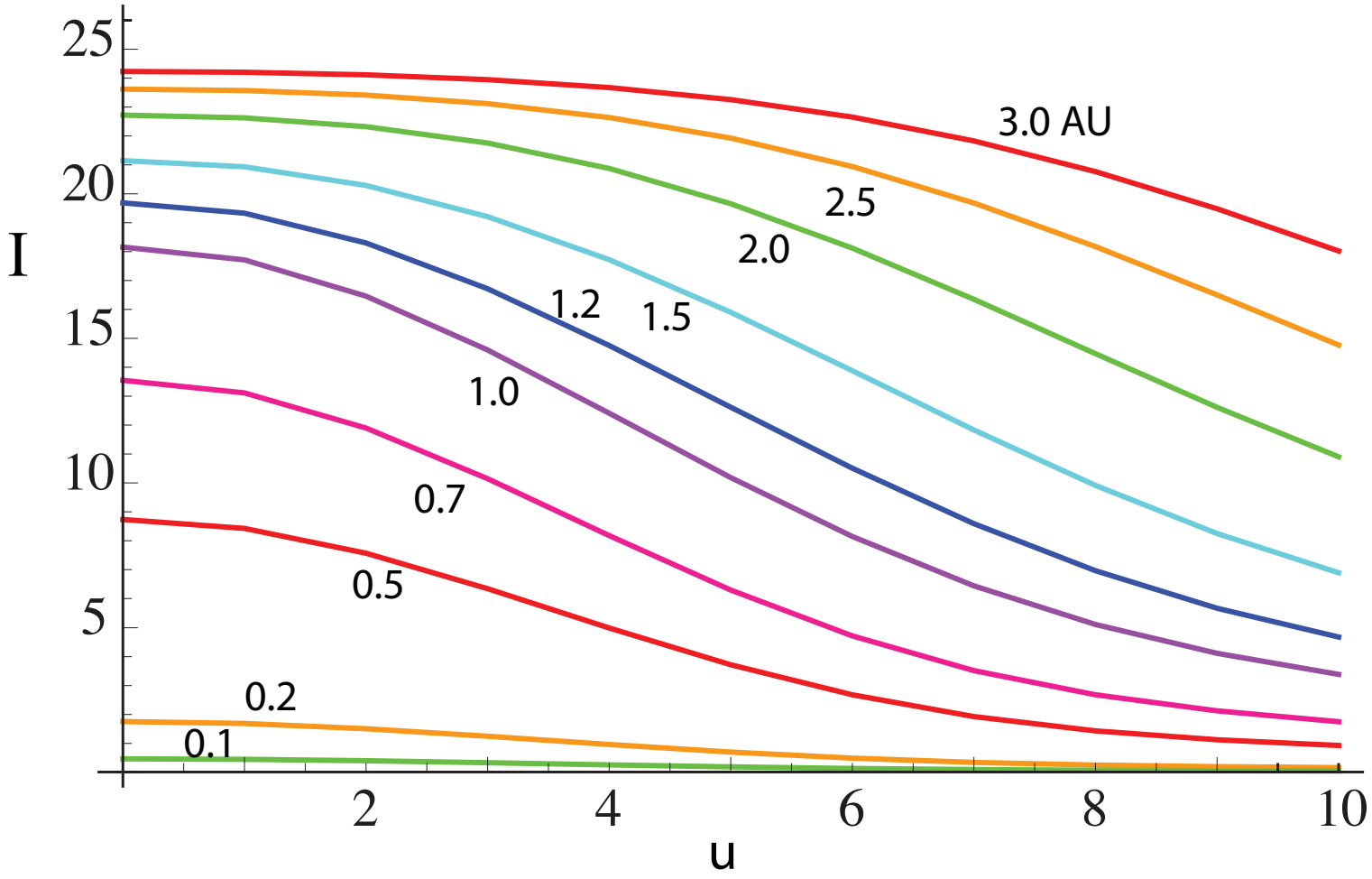

Optical sectioning with finite sized detector

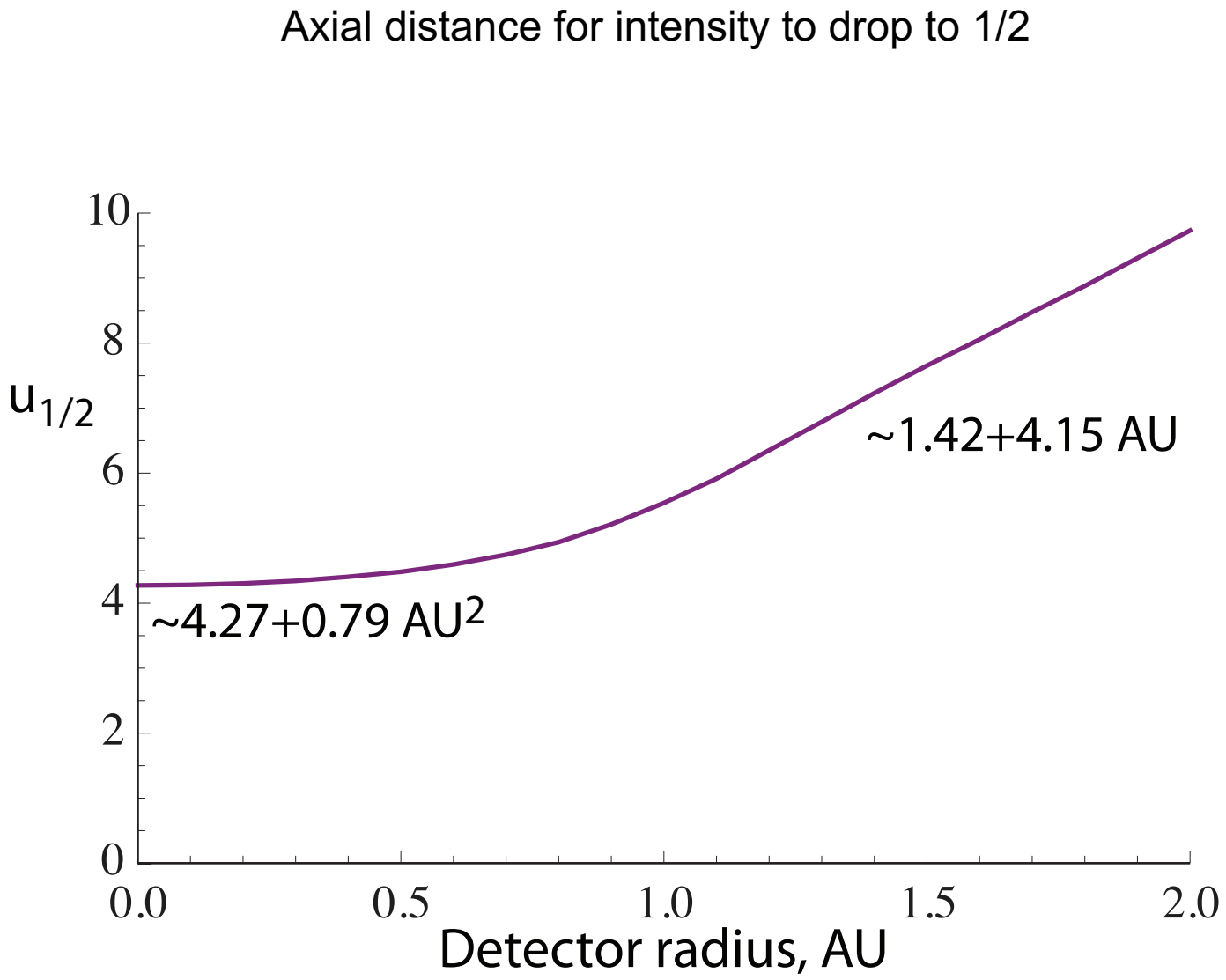

Improvements in resolution

System	Resolution improvement factor	Peak intensity
Conventional	1	1
Confocal (or ISM small array), Airy disk illumination [4]	1.39	0
Confocal (or ISM small array), Sonine filter [3, 26]	1.59	0
Confocal (or ISM small array), Bessel illumination [4]	1.72	0
ISM 1 AU array [21]	1.49	1.64
ISM large array, $a = 1/2$ [21]	1.53	1.84
ISM 1.355AU array, optimum a	1.52	1.81
ISM 2AU array, optimum a	1.53	1.92
ISM Bessel 0.836 AU array	1.82	1.28
2-photon, nonconfocal	0.69	0.54
2-photon ISM, 2 AU array	1.29	1.67
2-photon Bessel, nonconfocal	0.99	-
2-photon Bessel ISM, 2 AU array	1.49	-
3-photon, nonconfocal	0.57	0.35
3-photon ISM, 2 AU array	1.19	1.43

3. C. J. R. Sheppard, M. Castello, G. Tortarolo, G. Vicidomini, and A. Diaspro, "Image formation in image scanning microscopy, including the case of two-photon excitation," J. Opt. Soc. Am. A **34**, 1339–1350 (2017).
4. C. J. R. Sheppard and A. Choudhury, "Image formation in the scanning microscope," Opt. Acta **24**, 1051–1073 (1977).
21. C. J. R. Sheppard, S. B. Mehta, and R. Heintzmann, "Superresolution by image scanning microscopy using pixel reassignment," Opt. Lett. **38**, 2889–2892 (2013).
26. C. J. R. Sheppard, "Optimization of pupil filters for maximal signal concentration factor," Opt. Lett. **40**, 550–553 (2015).

Discussion

- Structured illumination can give improved resolution (x2)
- Confocal microscopy gives improved resolution but spatial frequency response at high spatial frequencies is low ($\times\sqrt{2}$ in PSF)
- But signal is also low, so must open pinhole, giving almost no improvement in resolution
- Pixel reassignment increases signal collection efficiency
- Also gives improved resolution, better than confocal
- And speed is increased
- ISM with 2 photon excitation improves resolution
- ISM with pupil filters can improve high frequency response